ELSEVIER

Palaeogeography, Palaeoclimatology, Palaeoecology 145 (1999) 259–302

PALAEO

Sequence stratigraphic interpretations from palynofacies, dinocyst and lithological data of Upper Eocene–Lower Oligocene strata in southern Mississippi and Alabama, U.S. Gulf Coast

Carlos A. Jaramillo [a,*], Francisca E. Oboh-Ikuenobe [b]

[a] *Paleobotany Laboratory, Florida Museum of Natural History, University of Florida, Gainesville, FL 32611, USA*
[b] *Department of Geology and Geophysics, University of Missouri–Rolla, Rolla, MO 65409-0410, USA*

Received 25 February 1998; accepted 6 July 1998

Abstract

This paper presents new information on the sequence stratigraphy of the Upper Eocene–Lower Oligocene strata in southern Mississippi and Alabama, based on palynological and lithological data from five sections. By integrating lithological characteristics with palynofacies assemblages, several dinocyst paleoecological groups, the *Deflandrea* group, and the abundance of reworked dinocysts in samples, paleobathymetric curves were reconstructed and used to revise the sequence stratigraphy of the area. We identified a maximum flooding surface in the middle of the Shubuta Clay Formation in southern Mississippi, and dated it as latest Eocene. In southern Alabama, the Eocene–Oligocene boundary was placed within a condensed section representing about 0.19 Ma, and it coincided with the Shubuta Clay–Vicksburg Group contact. This condensed section is equivalent to the accumulation of the upper Shubuta and Red Bluff Formations in southern Mississippi. The Forest Hill–Mint Spring contact, which has been interpreted as a sequence boundary that merged with a transgressive surface, does not correlate with the Tejas A (TA) 4.3/4.4 sequence boundary of Haq et al. (1988). The Pachuta Marl and lower Shubuta Clay Formations are constituents of a Late Eocene transgressive systems tract in southern Mississippi, but this systems tract extended to the Shubuta Clay–Vicksburg Group contact in southern Alabama. The overlying Early Oligocene highstand systems tract consisted of the upper Shubuta (in Mississippi), and the Red Bluff–Bumpnose–Forest Hill Formations. A thin sandstone in the Mint Spring was interpreted as a deposit of a possible lowstand systems tract above the sequence boundary in one southern Mississippi section. In general, the Mint Spring Marl and Marianna Limestone constituted a transgressive systems tract. © 1999 Elsevier Science B.V. All rights reserved.

Keywords: dinoflagellates; palynofacies; graphic correlation; paleoecology; sequence stratigraphy; U.S. Gulf Coast

1. Introduction

Outcrops of some of the most complete Upper Eocene to Lower Oligocene sedimentary rock sequences in North America are located in southern Mississippi and Alabama (Fig. 1) in the U.S. Gulf Coast. They have been the subject of several sequence stratigraphic, paleogeographic, magnetostratigraphic and biostratigraphic studies (e.g., Hazel et al., 1980; Siesser et al., 1985; Miller et al., 1993; Tew and Mancini, 1995; Pasley and Hazel,

* Corresponding author. Fax: +1 (352) 392-2539;
E-mail: carlos@flmnh.ufl.edu

0031-0182/99/$ – see front matter © 1999 Elsevier Science B.V. All rights reserved.
PII: S0031-0182(98)00126-6

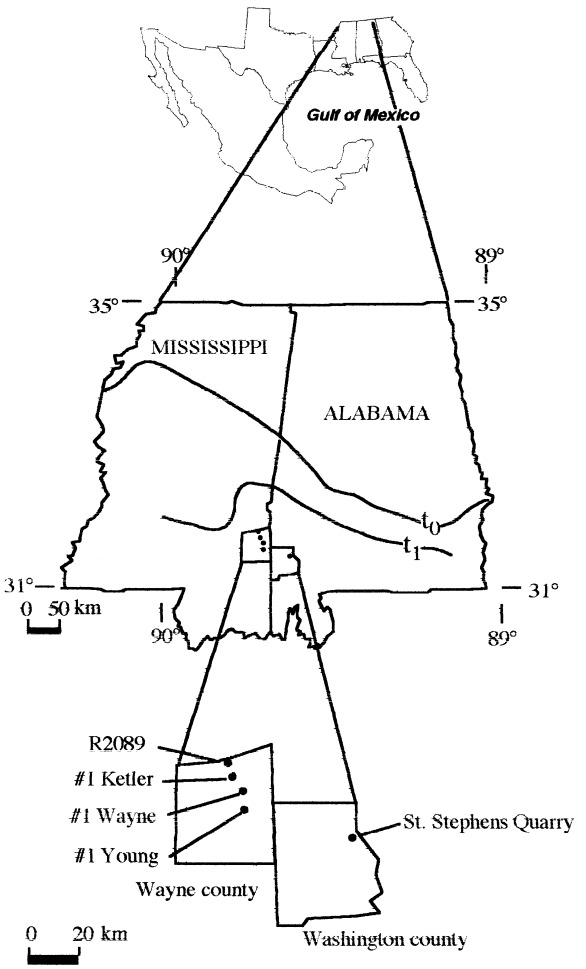

Fig. 1. Location of the studied localities in southern Mississippi and Alabama. t_0 corresponds to the paleoshoreline during the accumulation of the Shubuta Clay and equivalent units, while t_1 represents the paleoshoreline during the accumulation of the Red Bluff Clay and equivalent units (paleoshorelines after Tew and Mancini, 1995).

1995). One section in particular, the St. Stephens Quarry in southwestern Alabama, has been the most studied, providing controversial information on the position of the Eocene–Oligocene boundary and the sequence stratigraphic interpretation of the section, based on foraminiferal and calcareous nannoplankton biostratigraphy, magnetostratigraphy, stable isotope stratigraphy and lithostratigraphy (Mancini, 1979; Bybell, 1982; Siesser, 1983; Loutit et al., 1983, 1988; Keller, 1985; Baum and Vail, 1988; Pasley and Hazel, 1990, 1995; Miller et al., 1993; Tew and Mancini, 1995). Whereas the various sequence stratigraphic models proposed by these studies largely agree on many issues, the most notable discrepancies occur in the interpretation of the interval comprised by the Shubuta Clay, Bumpnose Limestone–Red Bluff Clay–Forest Hill Sand, Mint Spring Marl, and the Eocene–Oligocene boundary (Fig. 2).

The absence of good outcrop exposures in the area has resulted in the numerous studies focusing only on the few available outcrops. The different chronostratigraphic and sequence stratigraphic hypotheses proposed by these workers (Figs. 1 and 2) could be tested on new stratigraphic sections, such as the three recently drilled cores (#1 Young, #1 Wayne, #1 Ketler; Dockery et al., 1994) studied here. Palynofacies analysis, dinoflagellate cysts, and lithological data from these three cores and two outcrop sections (St. Stephens Quarry and R2089 Type Red Bluff) are used to: (1) propose a sequence stratigraphic interpretation for the area; and (2) locate the Eocene–Oligocene boundary. Other workers have demonstrated the usefulness of palynological data (in particular, palynofacies and dinoflagellate cysts) in identifying depositional environments and relative sea level changes, as well as attempting chronological correlation in marginal marine and neritic environments (Habib and Miller, 1989; Gregory and Hart, 1992; Brinkhuis, 1994; Dale, 1996). In the U.S. Gulf Coast, however, there is little published information on the dinoflagellate cysts in the Upper Eocene–Lower Oligocene units in spite of their extraordinary abundance, diversity and good preservation in the sediments.

2. Geologic setting

The Cenozoic history of the northwestern Gulf of Mexico is characterized by rapid ongoing sediment input and thick, prograding depositional sequences, which intertongue with interdeltaic shelf-edge sediments (Galloway, 1989). These units were deposited in a shallow marine to marginal marine setting of a passive margin. In general, Upper Eocene sediments are characterized by fine-grained sediment deposition, whereas the Lower Oligocene constitutes one of the great progradational wedges in the northwestern Gulf of Mexico (Galloway, 1989).

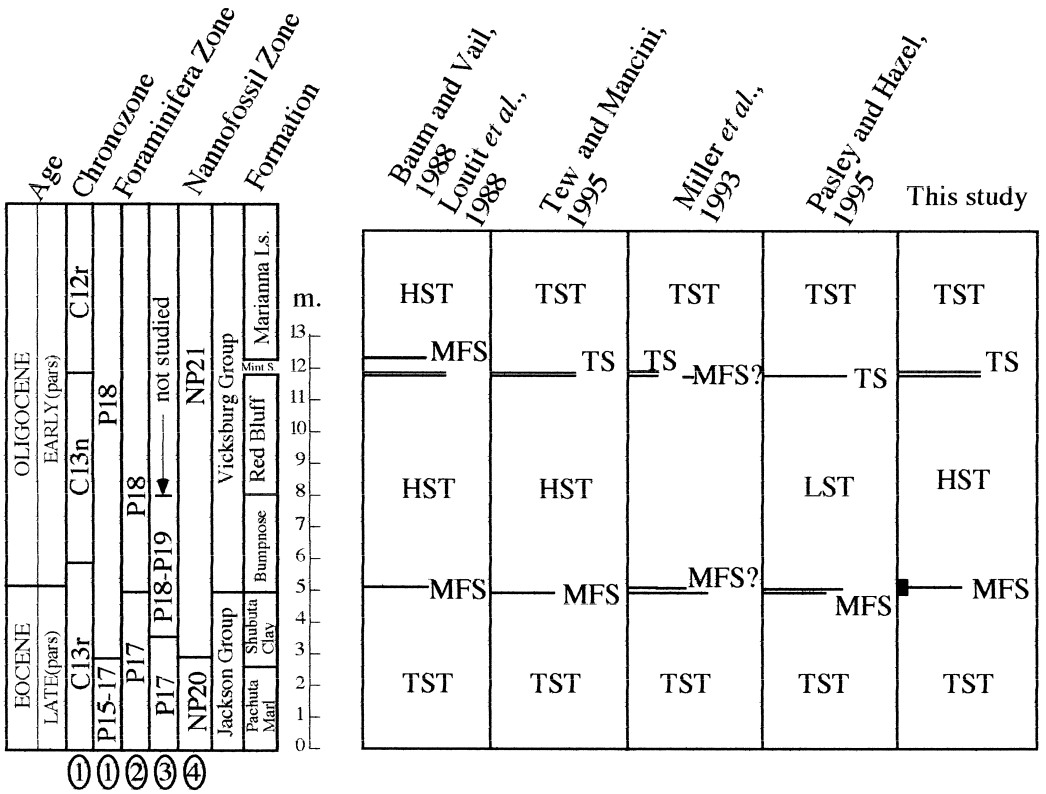

Fig. 2. Sequence stratigraphic, biostratigraphic and magnetostratigraphic interpretations of the St. Stephens Quarry section. Numbers 1–4 correspond to the following references: *1* = Miller et al. (1993); *2* = Mancini (1979); *3* = Keller (1985); *4* = Bybell (1982). See discussion in the text for the location of the Eocene–Oligocene boundary.

There are two uppermost Eocene lithostratigraphic units in southern Mississippi and Alabama: these are the Pachuta Marl and Shubuta Clay, both of the Jackson Group (Fig. 3). The lowest Oligocene strata consist of five lithostratigraphic units of the Vicksburg Group, namely the Bumpnose Limestone, Red Bluff Clay, Forest Hill Sand, Mint Spring Marl, and the Marianna Limestone. The Bumpnose Limestone, Red Bluff Clay and Forest Hill Sand are lateral equivalents of each other, with the Bumpnose and Red Bluff intertonguing in some areas in southwestern Alabama (Tew and Mancini, 1995) (Fig. 3). These lithostratigraphic units were deposited in a shallow marine to marginal marine setting of a passive margin.

Five different sequence stratigraphic models (including the one from this study) have been proposed for the St. Stephens Quarry section (Fig. 2; Baum and Vail, 1988; Loutit et al., 1988; Miller et al., 1993; Pasley and Hazel, 1995; Tew and Mancini, 1995). In general, the following facts have been recognized: (1) the Shubuta–Bumpnose contact corresponds to a maximum flooding surface; and (2) a sequence boundary is located at the base of the Mint Spring Marl. Miller et al. (1993) indicated that the Shubuta–Bumpnose contact corresponded to a sequence boundary, based on correlation to the TA 4.4 cycle boundary and a $\delta^{18}O$ increase at the contact. However, Loutit et al. (1988, fig. 21) reported a decrease of $\delta^{18}O$ at the same level. Pasley and Hazel (1995) proposed a sequence boundary immediately overlying a maximum flooding surface at the top of the Shubuta Clay. They also indicated that the Bumpnose Limestone and Red Bluff Clay were constituents of a lowstand systems tract, and that a sequence boundary was absent at the base of the Mint Spring Marl.

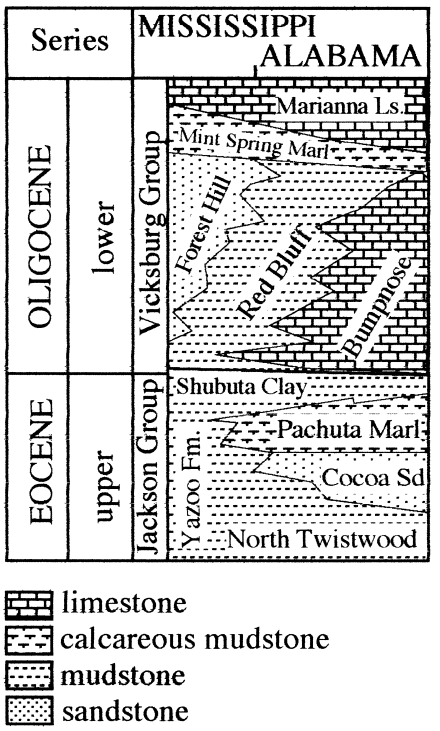

Fig. 3. Simplified stratigraphic correlation chart of Upper Eocene–Lower Oligocene sedimentary rocks in the Mississippi–Alabama area (modified from Galloway et al., 1991, and Pasley and Hazel, 1995).

3. Methods

We studied five Upper Eocene–Lower Oligocene localities in southern Mississippi and Alabama: three cores and one outcrop in southern Mississippi (#1 Young, #1 Ketler, #1 Wayne, and R2089 Type Red Bluff) and one outcrop section in southern Alabama (St. Stephens Quarry) (Fig. 1). Palynological samples for this study were derived from two sources: the U.S. Geological Survey (Reston, Virginia), which provided 40 processed, oxidized, palynological samples from the St. Stephens Quarry and R2089 sections; and Mobil Exploration and Production Services (Dallas, Texas), which provided 120 unoxidized and oxidized samples from the #1 Young, #1 Ketler, and #1 Wayne cores. Samples for palynologic work were prepared by the standard procedure of digesting the sediments in mineral acids (Traverse, 1988). Up to 300 dinocyst specimens were counted per sample with a Zeiss transmitted light microscope, to determine the taxonomic composition and abundance of the dinocyst community. The resulting dinocyst ranges for each location were then correlated using the technique of graphic correlation. The dinocyst distribution was also analyzed using multivariate techniques. The taxonomy of dinoflagellate cysts follows that cited in Lentin and Williams (1993) and Stover and Williams (1995). Previously undescribed species are given an informal classification (e.g., *Pentadinium* sp. A). The most important taxa used for paleoecological interpretation and graphic correlation are illustrated in Plates I–III. The palynological slides are currently in the possession of the junior author.

The unoxidized #1 Young samples provide the main data set for the palynofacies aspect of this study, because the oxidation process alters the natural colors of dispersed organic matter (palynodebris) and destroys certain types, such as structureless amorphous material. One slide per sample was scanned at about 20× in order to identify at least 300 organic matter particles. In the absence of a standard palynofacies classification systems, we have used a classification system (Table 1) adapted from Lorente (1986), Van Vergen et al. (1990), Oboh (1992), and Jaramillo (1995). An Euclidean-distance cluster analysis with average linkage, which is a multivariate technique, was performed on the palynodebris percentage data (Table 2) and used to develop a palynofacies model, which was then correlated with relative sea level changes. The Euclidean distance is especially designed to work with continuous or ratio scales (Systat, 1992). Moreover, the linkage averages all distances between pairs of objects in different clusters and decides how far apart they are (Sokal and Michener, 1958).

4. Palynofacies analysis

Generally, the dispersed organic matter content of sediments from neritic and marginal marine environments consists of two main components: organic matter derived from the continent (terrestrial in our classification, see Table 1), and organic matter produced in the ocean (such as dinoflagellate cysts and marine amorphous organic matter). Since the terrestrially derived, organic matter particles behave like

Table 1
Organic matter classification [a]

Category	Palynodebris	Description
Aquatic (structureless)	Structureless amorphous material	Gel-like and exhibit a 'clotted' appearance (Lorente, 1986).
Aquatic (structured)	Dinoflagellate cysts and foraminiferal wall linings	Marine microphytoplankton and chitinous internal linings of foraminifera; linings usually spirally coiled.
Terrestrial (structureless)	Resins	Unstructured amber-color fragments normally derived from stem tissues of gymnosperms.
	Black debris	Opaque particles without internal structure; have sharp angular edges or are lath-shaped; called black wood, charcoal or inertinite by several workers.
	Yellow–brown fragments	Structureless particles of yellow to light brown color attributed to highly degraded herbaceous material.
	Black–brown fragments	Unstructured dark brown material, which is attributed to highly degraded woody material.
Terrestrial (structured)	Cuticles	Cutin layer covering the epidermis of higher plants; usually well preserved and shows epidermis outline.
	Plant tissue	This group includes all other herbaceous material, with the exception of cuticles; collenchyma and parenchyma are included here.
	Woody material	Brown particles with sharp angular edges and/or discernible cellular structure.
	Pollen and spores	Spores belonging to pteridophytes and pollen of gymnosperms and angiosperms; sporomorphs are dispersed by water and wind into continental and marine environments (Muller, 1959; Traverse and Ginsburg, 1966).
	Fungi	This group includes all fungal remains, such as hyphae, mycelia and non-embryophitic spores.

[a] Adapted from Lorente (1986), Van Vergen et al. (1990), Oboh (1992) and Jaramillo (1995).

a clast in water, their relative proportions will decrease as the distance from the source increases. This is the basis for using palynofacies as indicators of variations in the distance to the shoreline, which ultimately can be related to changes in relative sea level. However, stochastic events such as retransporting of organic matter by oceanic currents and storms, pollen and spores transported by the wind, as well as changes in run-off and climate, can also have an influence on the organic matter content of sediments (Batten, 1996).

Using the core depth as scale, the relative frequencies of the organic matter types in the #1 Young core are plotted in Fig. 4. Lithological observations and geophysical logs (gamma ray, spontaneous potential, and resistivity) were used to reconstruct the stratigraphic section on the left-hand side of the figure. Euclidean-distance cluster analysis identified four groups of samples on the basis of their organic matter content (Figs. 4 and 5). In Group 1, the palynofacies assemblage is dominated by high content of structureless amorphous material, whereas Group 2 samples are rich in yellow–brown material, pollen and plant tissue. The palynofacies assemblage in Group 3 is dominated by black–brown fragments, black debris and plant tissue, while dinoflagellate cysts, black debris, black–brown fragments and pollen dominate in Group 4 samples. These groups were used for constructing a relative paleobathymetric curve for the core.

The paleobathymetric curve shows the relative movements of the shoreline during the latest Eocene and Early Oligocene. In order to construct the curve, the sample groups were organized into a lateral palynofacies sequence from the deepest to the shallowest depositional environments as follows: Group 1, Group 4, Group 2 and Group 3 (Fig. 5). Group 1 probably accumulated in the deepest environments (of the stratigraphic section), because high contents of structureless amorphous material are indicative of marine, probably deep offshore environments (Lorente, 1986; Pasley and Hazel, 1990). Group 4 has a high diversity of dinoflagellate cysts, combined with terrestrial material. A diverse dinoflagellate cyst

PLATE I

1. *Achomosphaera alcicornu* (Eisenack, 1954) Davey and Williams, 1966. 90 μm long, dorsoventral view, high focus, slide R2070T-1, St. Stephens Quarry (SSQ).
2. *Apteodinium australiense* (Deflandre and Cookson, 1955) Williams, 1978. 72 μm long, ventral view, low focus, slide 199.5-200, #1 Young.
3. *Batiacasphaera compta* Drugg, 1970. 65 μm long, lateral view, mid-focus, slide 384-384.5, #1 Young.
4. *Enneadocysta arcuata* (Eaton, 1971) Stover and Williams, 1995. 75 μm long, dorsoventral view, low focus, slide 344-344.5, #1 Young.
5. *Enneadocysta multicornuta* (Eaton, 1971) Stover and Williams, 1995. 60 μm long, dorsoventral view, low focus, slide 329.5-330, #1 Young.
6. *Cannosphaeropsis* sp. A 105 μm, high focus, slide 344-344.5, #1 Young.
7. *Corrudinium incompositum* (Drugg, 1970) Stover and Evitt, 1978. 42 μm, high focus, slide S2043F-cc, SSQ.
8. *Glaphyrocysta* sp. 57 μm long, dorsal view, mid-focus, slide 249.5-250, #1 Young.
9. *Elytrocysta* sp. A of Head and Norris, 1989. 40 μm long, dorsoventral view, high focus left, mid focus right, slide R2070J-1, SSQ.
10. *Cordosphaeridium inodes* (Klumpp, 1953) Eisenack, 1963. 100 μm long, dorsoventral view, low focus, slide R2071A-2, SSQ.
11. *Systematophora* sp. A. 70 μm long, dorsal view, mid focus, slide 239.5-240, #1 Young.
12. *Cribroperidinium tenuitabulatum* (Gerlach, 1961) Lentin and Williams, 1993. 58 μm long, ventral view, high focus, slide 349.5-350, #1 Young.
13. *Hemiplacophora semilunifera* Cookson and Eisenack, 1965. 53 μm long, dorsal view, mid-focus, slide 349.5-350, #1 Young.

PLATE II (see p. 266)

1. *Impagidinium dispertitum* (Cookson and Eisenack, 1965) Stover and Evitt, 1978. 45 μm long, ventral view, high focus, slide 309-309.5, #1 Young.
2. *Homotryblium plectilum* Drugg and Loeblich Jr. 1967. 60 μm wide, apical view, low focus, slide 329.5-330, #1 Young.
3. *Hystrichokolpoma rigaudiae* Deflandre and Cookson, 1955. 70 μm long, dorsal view, mid-focus, slide 378-378.5, #1 Young.
4. *Membranophoridium aspinatum* Gerlach, 1961. 120 μm long, dorsoventral view, high focus, R2070R-1, SSQ.
5. *Operculodinium aff. centrocarpum* 65 μm, mid-focus, slide 329.5-330, #1 Young.
6. *Lingulodinium siculum* (Drugg, 1970) Wall and Dale in Wall et al., 1973. 70 μm long, dorsoventral view, mid-focus, slide 384-384.5, #1 Young.
7. *Operculodinium placitum* Drugg and Loeblich Jr., 1967. 45 μm long, dorsal view, high focus, slide R2070L-2, SSQ.
8. *Pentadinium laticinctum* subsp. *laticinctum* Gerlach, 1969; emend Benedek et al., 1982. 88 μm long, ventral view, high focus, slide R2070R-1, SSQ.
9. *Pentadinium* sp. A. 70 μm, high focus, slide 199.5-200, #1 Young.
10. *Spiniferites pseudofurcatus* (Klumpp, 1953) Sarjeant, 1970; emend Sarjeant, 1981. 80 μm wide, antapical view, high focus, slide 344-344.5, #1 Young.
11. *Nematosphaeropsis pusulosa* (Morgenroth, 1966) Stover and Williams, 1987. 120 μm, low focus, slide R2070AD-1, SSQ.
12. *Spiniferites ramosus* (Ehrenberg, 1838) Mantell, 1854. 60 μm long, dorsal view, high focus, slide 309-309.5, #1 Young.
13. *Systematophora placacantha* (Deflandre and Cookson, 1955) Davey et al., 1969; emend May, 1980. 90 μm long, ventral view, high focus, slide 319.5-320, #1 Young.

PLATE III (see p. 267)

1. *Trigonopyxidia fiscellata* de Coninck, 1986. 55 μm long, dorsal view, low focus, Slide R2070D-1, SSQ.
2. *Deflandrea phosphoritica* Deflandre, 1938. 110 μm long, ventral view, mid-focus, slide 188.5-189, #1 Young.
3. *Charlesdowniea coleothrypta* (Williams and Downie, 1966) Lentin and Williams, 1976. 125 μm long, ventral view, mid focus, slide R2071D-1, SSQ.
4. *Deflandrea heterophlycta* Deflandre and Cookson, 1955. 150 μm long, dorsal view, low focus, slide S2043F-cc, SSQ.
5. *Tectatodinium pellitum* Wall 1967 emend. Head 1994. 48 μm wide, antapical view, mid-focus, slide R2070K-1, SSQ.
6. *Wetzeliella lobisca* (Williams and Downie, 1966) Jolley and Spinner, 1989. 160 μm long, ventral view, low focus, slide 344-344.5, #1 Young.
7. *Wetzeliella* sp. A. 124 μm long, dorsoventral view, mid-focus, slide 304-304.5, #1 Young.
8. *Ascostomocystis potane* Drugg and Loeblich Jr., 1967. 120 μm long, dorsoventral view, mid-focus, slide 279.5-280, #1 Young.
9. *Wetzeliella symmetrica* Weiler, 1956. 150 μm long, ventral view, mid-focus, slide 334-334.5, #1 Young.
10. *Cyclopsiella vieta* Drugg and Loeblich Jr., 1967. 100 μm long, dorsoventral view, mid-focus, slide R2070P-1, SSQ.

PLATE I

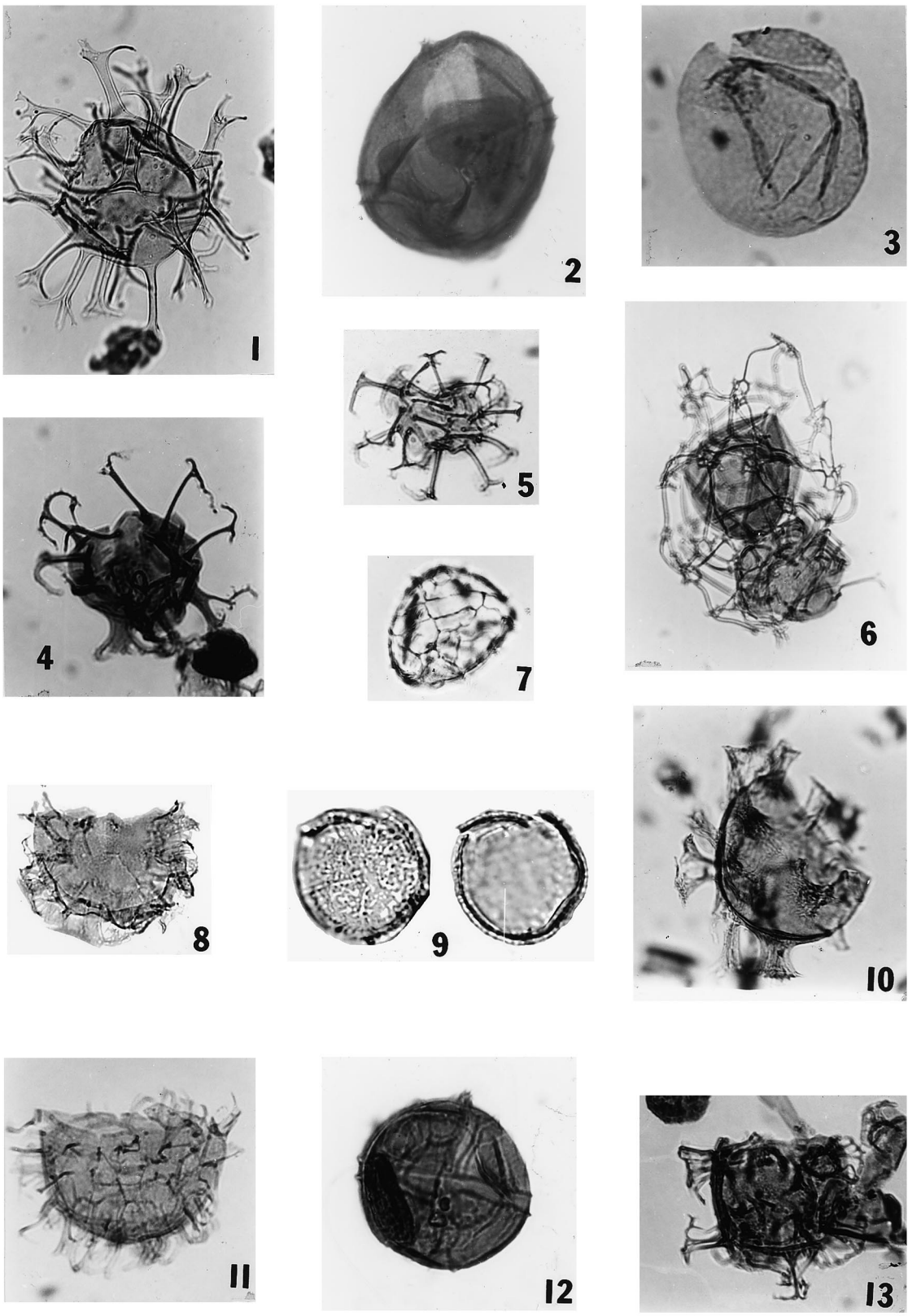

PLATE II

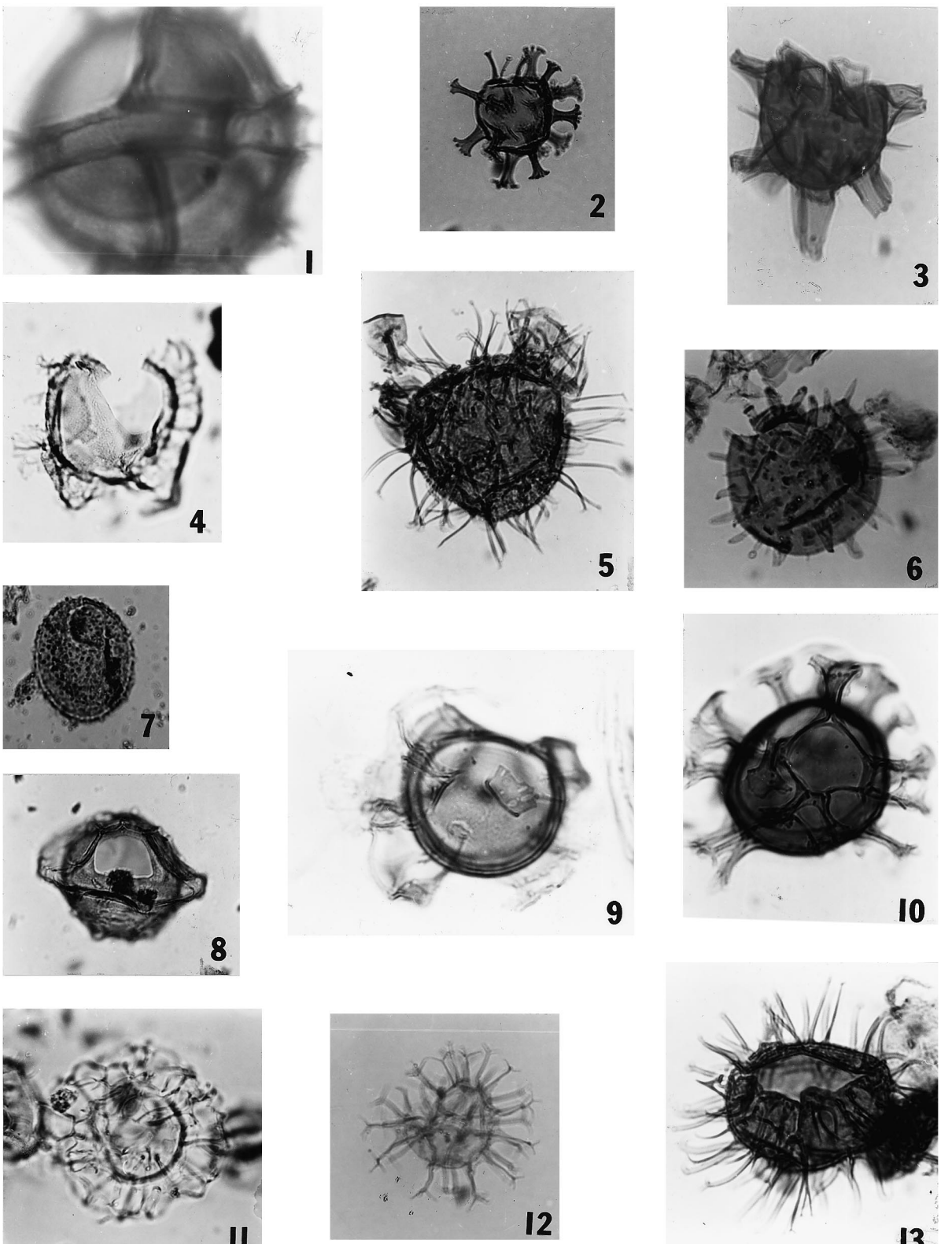

For description see p. 264.

PLATE III

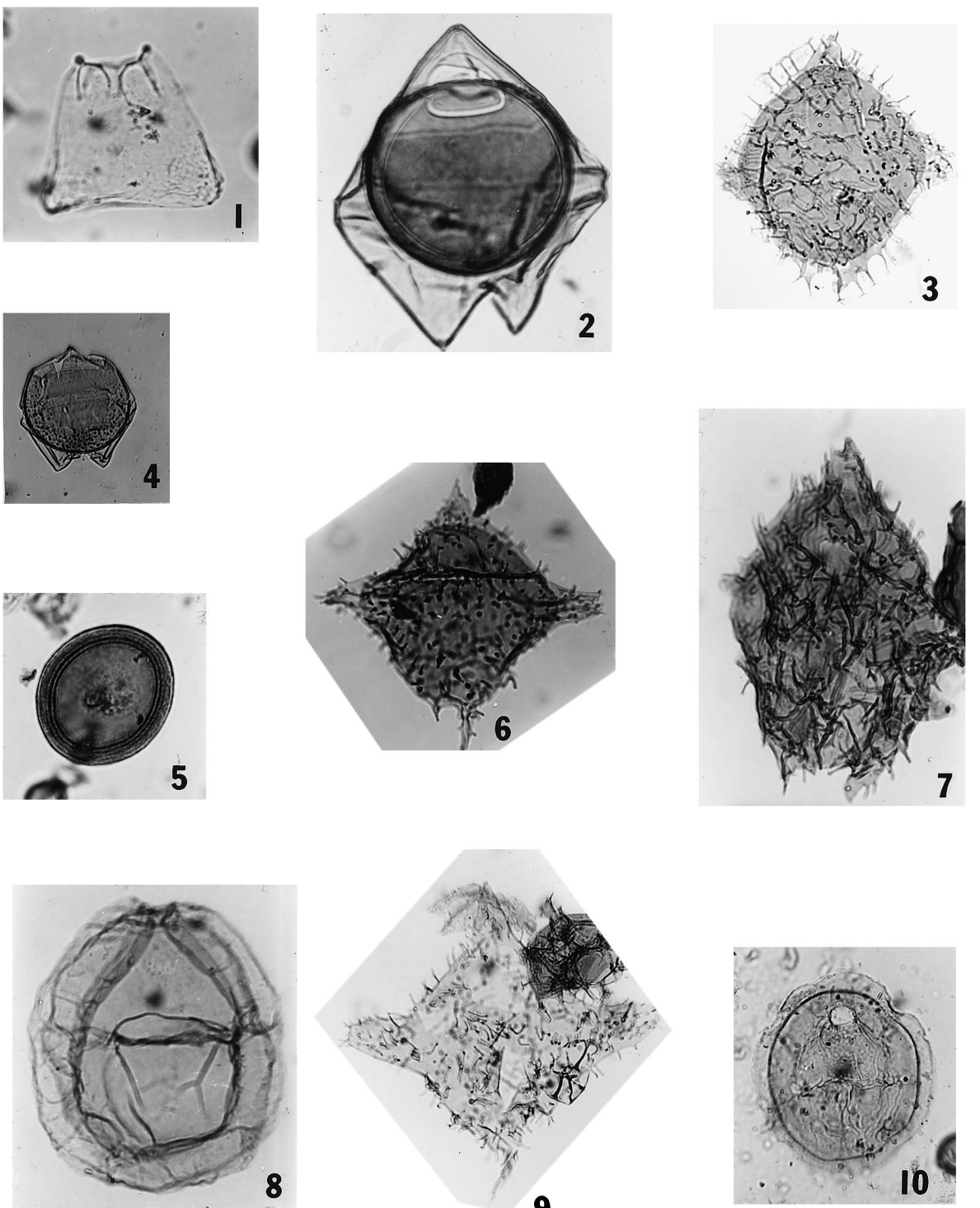

For description see p. 264.

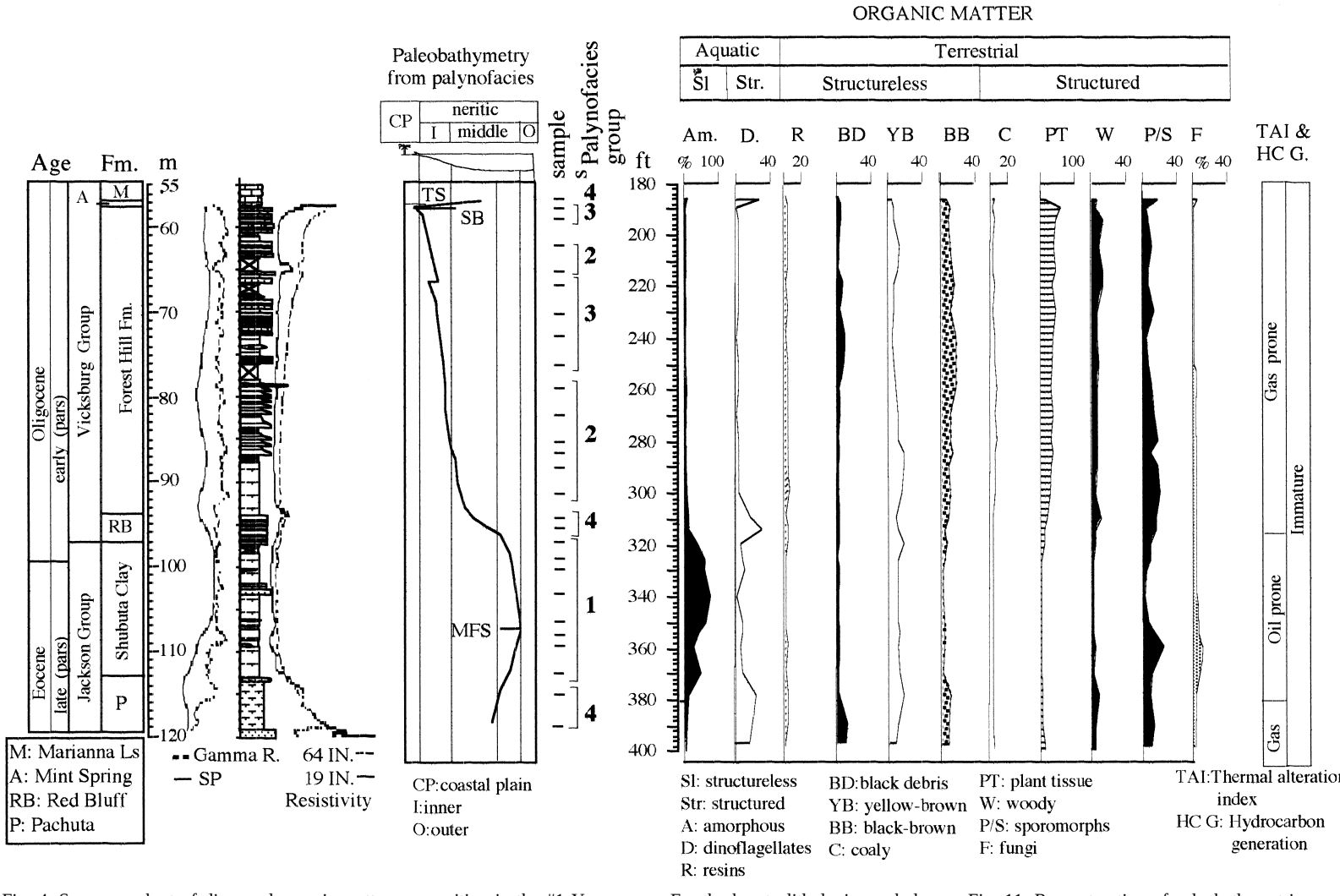

Fig. 4. Summary chart of dispersed organic matter composition in the #1 Young core. For the key to lithologic symbols, see Fig. 11. Reconstruction of paleobathymetric curve was based on the position of the palynofacies groups (identified from the cluster analysis) relative to the paleoshoreline. *TS* corresponds to transgressive surface, *SB* to sequence boundary, and *MFS* to maximum flooding surface.

Table 2
Palynodebris count data (%) for the #1 Young core

Sample (m)	Aquatic		Terrestrial								
	Structureless	Structured	Structureless				Structured				
	amorphous	dinocyst/for.	resins	black debris	yellow brown	black brown	cuticles	plant tissue	woody	sporom.	fungi
56.8	6.6	31.8	0.0	5.7	5.7	6.9	0.3	13.8	6.3	22.0	0.9
57.8	0.3	0.0	0.9	13.7	6.4	12.0	0.3	57.7	5.5	3.2	0.0
59.2	1.9	1.4	0.5	13.8	7.0	11.1	1.4	42.2	14.3	6.5	0.0
62.3	1.3	0.8	2.1	6.8	15.8	13.8	0.3	36.9	10.6	11.7	0.0
65.3	1.3	0.7	1.3	3.6	13.4	14.4	0.0	42.5	15.0	7.8	0.0
66.8	0.0	0.6	0.3	19.7	7.0	17.5	0.6	32.4	14.6	7.3	0.0
70	1.3	0.7	1.7	9.9	6.0	13.9	0.0	43.7	6.6	16.2	0.0
73.1	0.3	0.3	0.3	23.1	5.6	22.2	0.6	35.8	6.5	5.3	0.0
76.1	0.0	1.0	0.7	20.1	5.9	22.1	1.0	33.0	8.9	7.3	0.0
79.1	2.0	1.0	1.3	8.2	11.2	21.1	5.6	28.9	7.9	12.5	0.3
82.2	1.3	0.0	2.7	11.0	12.7	13.7	1.3	34.3	7.7	14.7	0.7
85.3	0.3	0.3	2.7	5.3	12.0	13.3	5.6	30.2	7.0	22.3	1.0
86.6	1.2	0.6	0.6	8.5	20.2	16.4	0.6	34.3	5.9	10.9	0.9
88.3	1.6	0.3	1.6	3.6	20.4	11.0	1.6	30.1	7.8	21.0	1.0
91.4	2.0	2.3	4.7	5.3	17.3	13.3	1.3	26.0	3.3	23.7	0.7
94.3	6.8	17.3	0.0	6.5	9.3	9.9	0.3	17.6	12.7	19.0	0.6
95.8	7.4	35.8	1.4	7.2	11.8	3.6	0.0	10.7	4.1	17.1	0.8
97.5	33.7	4.6	0.6	8.1	21.9	6.6	0.0	8.9	4.6	9.2	1.7
99.3	58.1	7.0	0.0	2.2	12.8	4.1	0.0	1.7	2.7	9.0	2.4
100.5	55.5	11.0	0.0	7.4	12.6	1.8	0.0	2.5	1.5	5.8	1.8
103.6	73.5	0.3	0.0	5.4	13.0	3.0	0.0	0.6	0.6	2.1	1.5
106.6	58.9	6.3	0.0	4.4	13.9	3.2	0.0	1.6	1.6	6.3	3.8
108	38.6	8.5	0.2	8.0	16.3	5.6	0.0	0.7	1.9	16.3	3.9
109.7	23.2	5.0	1.8	7.9	13.2	4.0	0.0	2.1	3.2	29.0	10.6
112.7	45.4	6.0	0.0	5.8	16.7	2.5	0.0	1.6	1.6	12.5	7.9
115.3	7.9	26.5	0.9	5.6	22.4	11.8	0.0	4.7	8.8	10.3	1.2
118.8	3.2	19.9	1.0	30.4	13.5	9.3	0.0	4.2	3.5	14.4	0.6

Organic matter categories are described in Table 1.

assemblage is common in shelf environments (Traverse, 1988); in this case, we interpret a possible inner to middle shelf, which is close enough to land to allow accumulation of terrestrially derived organic material. Group 2 is terrestrially influenced but still contains dinoflagellate cysts. This assemblage probably accumulated in an inner shelf environment. Finally, Group 3 represents the shallowest environment because it is comprised almost exclusively of terrestrially derived organic material. This group probably accumulated in the coastal plain–innermost shelf, transitional environment.

The entire #1 Young section is more or less considered gas prone due to the high content of terrestrial material. However, the interval from 97.3 m to 112.7 m (319.5–370 ft) is considered oil prone based on the high amount of amorphous organic matter (Fig. 4) (Lorente, 1986). The entire core section seems to be thermally immature.

5. Chronostratigraphy

A time-framework based on the stratigraphic distribution of dinoflagellate cysts (Tables 3–7) was developed, using graphic correlation (Shaw, 1964; Edwards, 1989). Several rounds of correlation were performed on all five stratigraphic sections in order to produce a standard composite section. The important fossil events in the composite section are

Table 3
Dinoflagellate cyst distribution in samples from the #1 Young core

Taxon	Meters from coretop down																			
	119	117	115	113	110	108	107	105	104	102	101	97.5	96.9	95.8	94	93	91	90	88	87
Achomosphaera alcicornu	2	5	9	25				2		9				5				1		1
Apteodinium australiense															1					
Enneadocysta arcuata							1	3		5	1	1								
Enneadocysta multicornuta							1	2		1	1	6								
Enneadocysta sp.													1							
Ascostomocystis potane							1			1	1		10	2	30	28	7	60	15	3
Azolla																				
Batiacasphaera aff. *baculata*				2																
Batiacasphaera baculata		1	2	2		1														
Batiacasphaera compta	177	28	3	1	1	1														
Cannosphaeropsis sp. A			2	1				1		1										
Elytrocysta sp. A of Head and Norris (1989)			1																	
Charlesdowniea coleothrypta	7	34	1	7	1	2	13	53	6	11	8	1	14	4		1				
Systematophora sp. A																				
Glaphyrocysta sp.										1										
Cleistosphaeridium sp. A		2		2		1	4			1					29			1	6	3
Cordosphaeridium cantharellum	1	1				1				1										
Cordosphaeridium gracile												1		1						
Cordosphaeridium inodes							1			2		1		2	1				2	1
Corrudinium incompositum	6		28	1	5							1	4	1	3					
Cribroperidinium tenuitabulatum		5	8	2		7	15	48	55	34	15	8	1				2		1	
Cyclopsiella vieta														1					1	
Dapsilidinium pseudocolligerum	2	6	2																	
Deflandrea heterophlycta					2					1			71	10		1		1		
Deflandrea phosphoritica	1	4	4				4		1	4			3	102		1		4	1	
Dinopterygium cladoides sensu Morgenroth		1	2				1	1		3										
Diphyes colligerum	2	4	2	3	1	5	6							1						
Distatodinium aff. ellipticum										1										
Hemiplacophora semilunifera		2				1	75	44		1										
Heteraulacacysta campanula										1			1							
Heteraulacacysta leptalea										1										
Histiocysta sp. A			1		1															
Homotryblium plectilum						1	116	10	184	15	211	185	49	21	1	1	7	60	94	175
Homotryblium vallum							2		2		3	5							2	6
Hystrichokolpoma cinctum			2																	
Hystrichokolpoma globulum?			1																	
Hystrichokolpoma rigaudiae	20	13	18	35	13	12	11	20	1	26	1			1	3		1			
Impagidinium dispertitum	3	4	10	5	2	2	1		6	1	3				7					
Impagidinium sp. A			1	1																
Impagidinium sp. B			1																	
Impagidinium sp. C																				
Lingulodinium pugiatum	1	4	2																	
Lingulodinium siculum	6	4	1			1				3		2			1					
Membranophoridium aspinatum																				
Muratodinium fimbriatum	2	2	1							1										
Nematosphaeropsis pusulosa															1					

Table 3 (continued)

Taxon	Meters from coretop down																			
	119	117	115	113	110	108	107	105	104	102	101	97.5	96.9	95.8	94	93	91	90	88	87
Operculodinium aff. *centrocarpum*	6	6	11	14	2	2	4	6	1	33	8	8	7	12	44	1			3	3
Operculodinium divergens											2									1
Operculodinium placitum															12					
Palaeocystodinium golzowense		2		1								1								
Pediastrum sp.													1			1		1	3	
Pentadinium laticinctum	1	6	6	1	2	1	7	20	33	14	4	22	26	4	2	1				
Pentadinium sp. A																				
Phthanoperidinium sp. A		3																		
Polysphaeridium cf. *zoharyi*																				
Polysphaeridium sp.																				
Pterospermella sp.																			1	
Rhombodinium draco			1	1																
Rottnestia borussica		2	2							5										
Samlandia clamydophora	6	3	2		4		1						4	1						
Spiniferites pseudofurcatus	1	3	6	42	1	18	4	7		8	4	1	1	2	20				2	
Spiniferites ramosus	49	150	161	24	15	16	10	7	5	13	8	5	5	1	135				9	1
Systematophora placacantha					2		19	73	2	87	26	15			1					
Tectatodinium pellitum											1	1	3		3					
Thalassiphora pelagica	1	1								3										
Trigonopyxidia fiscellata	1		6		3	3							1							
Valensiella? clathroderma	1		6	1	1	5														
Wetzeliella articulata																1				
Wetzeliella lobisca							1	1	1	1	1		2			1				1
Wetzeliella sp.	3								2		2		5	3				3	1	1
Wetzeliella symmetrica										1			1							
Spinidinium sp. A (RW)	2				1		2													
Lentinia sp. (RW)		5							1		3	1	1	7	1			2	2	2
Cerodinium sp. A (RW)							1													
Spiniferites ramosus subsp. *cavispinosus* (RW)										2										
Cyclonephelium sp. A (RW)										9										
Chatangiella sp. B (RW)																4		2		
Chatangiella sp. A (RW)																2			1	
Chichaouadinium sp. A (RW)																				
Muratodinium sp. (RW)																				
Circulodinium distinctum (RW)																				
Oligosphaeridium pulcherrimum (RW)																				
Alisogymnium euclaense (RW)			1																	
Veryhachium sp. A (RW)																3	1	4	1	
Palaeohystrichophora infusorioides (RW)																2			1	
Dinogymnium acuminatum (RW)																1				
Dinogymnium undulosum (RW)																		1		
Acritarch A (RW)																		2		1
Veryhachium sp. B (RW)																				
Acritarch B (RW)																				
Odontochitina sp. (RW)																				

Table 3 (continued)

Taxon	Meters from coretop down																		
	85	84	82	81	79	76	74	73	71	70	69	67	65	63	62	61	59	58	57
Achomosphaera alcicornu							1	2							2		1	1	2
Apteodinium australiense								1			1					1			
Enneadocysta arcuata								1											
Enneadocysta multicornuta																			
Enneadocysta sp.						2													
Ascostomocystis potane	70	271	41	57	31	125	24	46	10	1	95		1	1		2	1		
Azolla															1				
Batiacasphaera aff. *baculata*																			
Batiacasphaera baculata																			
Batiacasphaera compta																			
Cannosphaeropsis sp. A																			
Elytrocysta sp. A of Head and Norris (1989)																			
Charlesdowniea coleothrypta		1	2				3					1		2	1	2		14	1
Systematophora sp. A						1		3											
Glaphyrocysta sp.						2		24				1	2			1	1		
Cleistosphaeridium sp. A	1	1		11		26	8	30	1		4	69	2					6	3
Cordosphaeridium cantharellum				1				1											
Cordosphaeridium gracile		1																	
Cordosphaeridium inodes		5	1	2		1		4		1				2	1	1			1
Corrudinium incompositum																			
Cribroperidinium tenuitabulatum				1				1	1			1							
Cyclopsiella vieta																1	1	5	
Dapsilidinium pseudocolligerum																			
Deflandrea heterophlycta																		5	1
Deflandrea phosphoritica		1					1								16	1	1	195	150
Dinopterygium cladoides sensu Morgenroth	1																		
Diphyes colligerum																			
Distatodinium aff. ellipticum																			
Hemiplacophora semilunifera																			
Heteraulacacysta campanula																			
Heteraulacacysta leptalea																			
Histiocysta sp. A																			
Homotryblium plectilum	20	6	12	48	6	53	34	57	2	2	1	6	9	2	26	59	21		6
Homotryblium vallum								1											1
Hystrichokolpoma cinctum																			
Hystrichokolpoma globulum?																			
Hystrichokolpoma rigaudiae	1			1		1	1		1					1	4	4	2	13	12
Impagidinium dispertitum																			
Impagidinium sp. A																			
Impagidinium sp. B																			
Impagidinium sp. C			1																
Lingulodinium pugiatum																			
Lingulodinium siculum				1														1	15
Membranophoridium aspinatum				1				6				3				1			5
Muratodinium fimbriatum																			
Nematosphaeropsis pusulosa																			

Table 3 (continued)

Taxon	Meters from coretop down																		
	85	84	82	81	79	76	74	73	71	70	69	67	65	63	62	61	59	58	57
Operculodinium aff. *centrocarpum*	5	1	5	15		13	2	5	2		1		9	2	1	2	1	4	21
Operculodinium divergens				3									1		1				6
Operculodinium placitum																			
Palaeocystodinium golzowense							1												
Pediastrum sp.		2		1	1	5	3	3			1	1	3	2	2	3	2		
Pentadinium laticinctum			2	1		1	2	1		1	1	4	4	2	1	1	1		4
Pentadinium sp. A	1				1		1						89	47	14	75	45		
Phthanoperidinium sp. A																			
Polysphaeridium cf. *zoharyi*																	1		
Polysphaeridium sp.				1															
Pterospermella sp.	1													1					
Rhombodinium draco																			
Rottnestia borussica																			1
Samlandia clamydophora				1								2		1			1		2
Spiniferites pseudofurcatus		3		0	0	0	0	0	1	0	0	2	0	0	1		1	52	42
Spiniferites ramosus		1			4	15		14		1		6	1	3		7	1	2	1
Systematophora placacantha	1					1		10				2				5	1	1	21
Tectatodinium pellitum																			
Thalassiphora pelagica				1			1												1
Trigonopyxidia fiscellata																			
Valensiella? clathroderma																			
Wetzeliella articulata			1			1													
Wetzeliella lobisca			2			2							1					1	
Wetzeliella sp.		2		5			2	2	1		1								
Wetzeliella symmetrica		2				1							1						
Spinidinium sp. A (RW)								1							1		1		
Lentinia sp. (RW)	6		3	7			1	1				4					1	1	
Cerodinium sp. A (RW)	1	1					1												
Spiniferites ramosus subsp. *cavispinosus* (RW)		1								1	1								1
Cyclonephelium sp. A (RW)								2											
Chatangiella sp. B (RW)		1	5	3			4		2	1		1	1		1				
Chatangiella sp. A (RW)	1	1	2	5	2	3	5	3	2	2	5	4	1	1	2	2	1	1	
Chichaouadinium sp. A (RW)		1		1								1	1			1			
Muratodinium sp. (RW)				1		1						1		10					1
Circulodinium distinctum (RW)					1	1						1		1					
Oligosphaeridium pulcherrimum (RW)																			1
Alisogymnium euclaense (RW)		1		1							1	1	1						
Veryhachium sp. A (RW)	2	2	1		1	1	3	2	1	2			1	1	1		1		
Palaeohystrichophora infusorioides (RW)	3	2	2		1	1	2	2			1	5				1	1		
Dinogymnium acuminatum (RW)			1		1														
Dinogymnium undulosum (RW)															1				
Acritarch A (RW)	1			1			1								1				
Veryhachium sp. B (RW)	1			1									1	1					
Acritarch B (RW)					1	1													
Odontochitina sp. (RW)								1											

RW = reworked

Table 4
Dinoflagellate cyst distribution in samples from the St. Stephens Quarry section

Taxon	Meters from base up												
	2.7	3.2	4.7	5.0	5.3	6.0	6.8	8.7	10.0	11.7	11.9	12.3	19.7
Achomosphaera alcicornu	1	1		1	1								
Apteodinium australiense	4				1	1							
Enneadocysta arcuata	1	1				1							
Enneadocysta sp.			1										
Ascostomocystis potane			1	1	2								
Batiacasphaera baculata	1												
Batiacasphaera compta	1												
Elytrocysta sp. A of Head and Norris (1989)	16	2	108										
Charlesdowniea coleothrypta	1	3	1	3	1	1							
Cleistosphaeridium sp. A							5						
Cordosphaeridium cantharellum			1		1	1							
Cordosphaeridium inodes	1				1	1		1					
Corrudinium incompositum	54	11	25	1	1	3	156	1			18	18	
Cribroperidinium sp. A	1												
Cribroperidinium tenuitabulatum	1												
Cyclopsiella vieta				4	1	1	1	2	2		86	9	
Dapsilidinium pseudocolligerum						1	1						
Deflandrea heterophlycta	3	30	60	199	202	1	6					1	
Deflandrea phosphoritica	4	8	27	18	19	55	21	20	3	1	10	11	
Diphyes colligerum				1		2							
Hemiplacophora semilunifera			5										
Histiocysta sp. A	1	2	5	1		1					3	1	
Homotryblium plectilum	64	71	39	44	56	208	38	25	40	5	13	2	1
Homotryblium vallum				1	1	5	3	1	4				
Hystrichokolpoma rigaudiae			1			1							
Impagidinium dispertitum	16			1	1								
Impagidinium? simplicium	5												
Lejeunecysta hyalina		1				1							
Lingulodinium siculum					1	1							
Membranophoridium aspinatum				1		1	1						
Multispinula sp.													
Nematosphaeropsis pusulosa	1		2			1							
Operculodinium centrocarpum	1	1	2	4		7	16						
Operculodinium divergens					1					1	1		
Operculodinium placitum			2	6	1							1	
Palaeocystodinium golzowense	1	3						1			2		
Pediastrum sp.								2	2				
Pentadinium laticinctum	30	18	15	4	3	1	3	7		1	11	3	
Pentadinium laticinctum subsp. *granulatum*													
Pentadinium sp. A								20	6	1			
Pterospermella sp.	1		1				2						
Rhombodinium draco	1												
Rhombodinium sp.													
Samlandia clamydophora	1	1	1	3	7	2	5	1	1		3		
Spiniferites pseudofurcatus	8	4	2	1		1	7	4					10
Spiniferites ramosus	3	1	1	1	1	3	27	3	2				
Systematophora placacantha	2	3	1	1	1	1	5						51
Tectatodinium pellitum	12	1	2	5									
Thalassiphora delicata						1							
Trigonopyxidia fiscellata	20	1											
Wetzeliella lobisca			1										

Table 4 (continued)

Taxon	Meters from base up												
	2.7	3.2	4.7	5.0	5.3	6.0	6.8	8.7	10.0	11.7	11.9	12.3	19.7
Wetzeliella sp.		1	1	1	1								
Lanternosphaeridium sp. A (RW)							1						
Spiniferites ramosus subsp. *cavispinosus* (RW)							2	5					

Numbers are raw countings. RW = reworked.

shown in Table 8. The next step was to tie this composite section to worldwide chronostratigraphy. We did not use dinocyst datums for this task because there is no dinocyst zonation either worldwide or for the Gulf Coast. Secondly, the Eocene–Oligocene boundary is internationally defined on the basis of foraminifera.

The International Geological Congress held in Kyoto in 1992 defined the Eocene–Oligocene boundary by the last occurrence of *Hantkenina* spp. at the Massignano section in the Apennines (Italy). This datum is located in the youngest part of the magnetostratigraphic C13r (C13r.14) Chron and has an age estimated at 33.7 Ma (Berggren et al., 1995). This boundary coincides with the P17–P18 foraminiferal boundary if the upper boundary of the P17 zone is defined by the last occurrence of *Hantkenina* spp. Another important marker is the last occurrence of *Turborotalia cerroazulensis*, an important element of P17 zone, which is 0.1 Ma older than the Eocene–Oligocene boundary but eventually may be proved to be coeval with it (Berggren et al., 1995). The boundary is also within the nannoplankton NP21 zone. Brinkhuis and Visscher (1995) argue for redefining the Eocene–Oligocene boundary in the Priabonian type section (in Italy) to correspond with the lithological top of the Priabonian Stage. According to them, this would correlate with the TA 4.3/TA 4.4 sequence boundary of Haq et al. (1988) and the $\delta^{18}O$ increase event related to growth of an Antarctic continental sheet. We agree with the boundary defined at the Massignano section (Berggren et al., 1995), and do not follow Brinkhuis and Visscher's suggestion for the following conflicting reasons: (1) the Cycle chart of Haq et al. (1988) shows that the Eocene–Oligocene boundary corresponds to (or it is slightly below) the Chron C13r–C13n magnetoboundary, the top of P17 zone and the TA 4.3/TA 4.4 sequence boundary; (2) Baum and Vail (1988) and Loutit et al. (1988) identified the TA 4.3/TA 4.4 sequence boundary in the Gulf Coast at the Forest Hill–Mint Spring contact which is located above the Eocene–Oligocene boundary defined by foraminifera (see Figs. 2 and 6). Thus, there is a source of confusion because there is no agreement in the chart between the sequence boundary (TA 4.3/TA 4.4) and its alleged age (defined by foraminifera and magnetostratigraphy).

In the Priabonian section, Brinkhuis (1994) indicated that the Eocene–Oligocene boundary (as defined by the last occurrence of *Hantkenina*) would be located 15 m below the lithostratigraphic position of the TA 4.3/TA 4.4 sequence boundary. He used dinoflagellate cysts to correlate the position of the last occurrence of *Hantkenina* from the Massignano section since this foraminifer has not been found in the Priabonian section. However, even with this new interpretation of the chronological location of the Priabonian TA 4.3/TA 4.4 sequence boundary, the correlation with the sequence boundary at the Forest Hill–Mint Spring contact seems improbable because the Priabonian sequence boundary, once again by correlation with dinoflagellate cysts (Brinkhuis, 1994, fig. 4), would occur in the lower part of the Chron C13n instead of the C13n–C12r boundary as in the Gulf Coast (Fig. 6). Therefore, the Priabonian and Forest Hill–Mint Spring sequence boundaries are not coeval, and the TA 4.3/TA 4.4 sequence boundary may not be worldwide in occurrence and should not be used as a time line.

Pasley and Hazel (1995) proposed a sequence boundary at Shubuta–Red Bluff contact (Fig. 2) which they correlated with the TA 4.3/TA 4.4 sequence boundary by Haq et al. (1988) (of the Priabonian section). They argued that this sequence boundary would alleviate the confusion of its chronolog-

Table 5
Dinoflagellate cyst distribution in samples from the #1 Wayne core

Taxon	Meters from coretop down												
	61	56	52	47	43	38	33	29	24	17	9.5	6	3.1
Apteodinium australiense		1			1	1							
Enneadocysta arcuata	4	1	1	1									
Enneadocysta sp.	1												
Ascostomocystis potane	2		5	93	85	66	5	3	9	4	1		
Cannosphaeropsis sp. A	2												
Elytrocysta sp. A of Head and Norris (1989)	1												
Charlesdowniea coleothrypta	7	3				1							
Systematophora sp. A			1	2	1		1			1			
Glaphyrocysta sp.				6	1	1							
Cleistosphaeridium sp. A	11		11	4	2	1	7	15	2				
Cordosphaeridium gracile				1									
Cordosphaeridium inodes		2	13	1	6	1		1					
Corrudinium incompositum	1											1	5
Cribroperidinium tenuitabulatum	82	1	2					1					
Cyclopsiella vieta											1	17	11
Dapsilidinium pseudocolligerum	1											16	
Deflandrea heterophlycta												1	13
Deflandrea phosphoritica	1	4										47	13
Dinopterygium cladoides sensu Morgenroth	2												
Distatodinium aff ellipticum	1												
Hemiplacophora semilunifera	16												
Heteraulacacysta campanula						1		1					
Heteraulacacysta leptalea		2											
Homotryblium plectilum	4	265	128	157	76	3	21	7	5	3	2	5	3
Homotryblium vallum					1			1				1	
Hystrichokolpoma rigaudiae	6				1								4
Lingulodinium siculum	1											2	1
Membranophoridium aspinatum		3	2	3	1	3	5	2	1		4		
Operculodinium centrocarpum	4	3	16	7	3	3	1	1	1			3	11
Pentadinium laticinctum	5	2						1			1	33	1
Pentadinium laticinctum subsp. *granulatum*	1												
Pentadinium sp. A			2	22	1	1			1			1	
Samlandia clamydophora		1								1	1	54	
Spiniferites pseudofurcatus	2	1	2					3	1	1	1	16	14
Spiniferites ramosus	15	1	13	2		2	1				2	6	
Systematophora placacantha	114	1				1	1		2	1		11	
Tectatodinium pellitum	2												
Trigonopyxidia fiscellata	1												
Wetzeliella articulata	1					1				1			
Wetzeliella lobisca	7												
Wetzeliella sp.	9	1					1		1				
Wetzeliella symmetrica	7			1		1			1				
Palaeohystrichophora infusorioides (RW)			1										
Muratodinium sp. (RW)						1		1					
Odontochitina sp. (RW)						1							
Cyclonephelium sp. A (RW)							1		1				
Chatangiella sp. B (RW)								1		1	4		
Acritarch A (RW)									1				
Alisogymnium euclaense (RW)											1		
Lanternosphaeridium sp. (RW)					1							4	
Spiniferites ramosus subsp. *cavispinosus* (RW)					1							7	16
Oligosphaeridium pulcherrimum (RW)			1				1						

Table 5 (continued)

Taxon	Meters from coretop down												
	61	56	52	47	43	38	33	29	24	17	9.5	6	3.1
Dinogymnium acuminatum (RW)			1										
Chatangiella sp. A (RW)			2	1				2		1			
Veryhachium sp. A (RW)			1		3				1		1		

Numbers are specimens counted. RW = reworked.

Table 6
Dinoflagellate cyst distribution in samples in the #1 Ketler core

Taxon	Meters from coretop down						
	37	3.4	26	21	17	12.1	6
Achomosphaera alcicornu					3		
Enneadocysta arcuata				1			
Enneadocysta sp.					1		
Ascostomocystis potane							18
Batiacasphaera baculata		2					
Batiacasphaera compta	21	2			1		
Elytrocysta sp. A of Head and Norris (1989)				1	1		
Charlesdowniea coleothrypta	2	1	17			5	
Cleistosphaeridium sp. A		1			2		1
Corrudinium incompositum	1	1					1
Cribroperidinium tenuitabulatum			82	1		2	
Cyclopsiella vieta							1
Dapsilidinium pseudocolligerum					1		
Deflandrea heterophlycta			5	6			7
Deflandrea phosphoritica		1	6	1	1	2	3
Diphyes colligerum	1	1					
Hemiplacophora semilunifera					66	4	
Histiocysta sp. A					1		
Homotryblium plectilum	4				8	249	1
Hystrichokolpoma rigaudiae	1		1	1	11	1	
Impagidinium dispertitum			1		3		
Impagidinium? simplicium					3		
Operculodinium centrocarpum	5	3			2	2	1
Palaeocystodinium golzowense	1						
Pediastrum sp.							2
Pentadinium laticinctum	47	281	37	3	24	3	1
Phthanoperidinium sp.	1						
Pterospermella sp.							1
Rhombodinium draco		1					
Samlandia clamydophora	14	2			12	1	
Spiniferites pseudofurcatus	4	2	28	7	12		
Spiniferites ramosus	5	2	1		4		1
Systematophora placacantha					17	29	1
Tectatodinium pellitum					1		
Trigonopyxidia fiscellata	2	1	6	4			
Valensiella? clathroderma			5	5			
Wetzeliella sp.					4	3	1
Spiniferites ramosus subsp. *cavispinosus* (RW)			1				
Veryhachium sp. A (RW)					2		1

Numbers are specimens counted. RW = reworked.

Table 7
Dinoflagellate cyst distribution in samples from the R2089 section

Taxon	Meters from oldest sample								
	0.0	1.2	5.4	6.4	7.2	12.0	12.4	13.0	13.6
Achomosphaera alcicornu			1						
Enneadocysta multicornuta			1						
Enneadocysta sp.					1				
Ascostomocystis potane						1		1	3
Batiacasphaera aff. *baculata*			1						
Batiacasphaera compta	10								
Cannosphaeropsis sp. A			1						
Cerebrocysta bartonensis			12	14	1				
Charlesdowniea coleothrypta			1		2			1	
Corrudinium incompositum		1	1	3				6	
Cribroperidinium tenuitabulatum	1	3			10	1			
Dapsilidinium pseudocolligerum					1				
Deflandrea heterophlycta							2	274	4
Deflandrea phosphoritica		2	6	1	1	24	3		
Dinopterygium cladoides sensu Morgenroth			1		4				
Heteraulacacysta campanula			2	1		1			
Homotryblium plectilum		1	25	13	120	9	16	4	1
Hystrichokolpoma rigaudiae	1					2		1	
Impagidinium dispertitum							1		
Lejeunecysta hyalina				1					
Membranophoridium aspinatum								1	
Operculodinium placitum						1			
Palaeocystodinium golzowense						1			
Pediastrum							1	2	
Pentadinium laticinctum	3	1	10	4	6				4
Pterospermella	1					1		3	1
Samlandia clamydophora	1		1		2			4	
Spiniferites pseudofurcatus			2						
Spiniferites ramosus	2		1						
Systematophora placacantha			9	3	23			1	
Tectatodinium pellitum			1		5	1			
Trigonopyxidia fiscellata	1				1	1			
Wetzeliella sp.				1				1	1

Numbers are specimens counted.

ical location, because the paleontological boundary (defined by the last occurrence of *Hantkenina*) coincided with the Shubuta–Red Bluff contact. However, the above discussion shows that the paleontological Eocene–Oligocene boundary does not correspond with the TA 4.3/TA 4.4 sequence boundary in the Priabonian section (Fig. 6).

In this study, foraminiferal datums (last occurrence of *Hantkenina* spp. and *T. cerroazulensis*) were used to tie our composite section to worldwide chronostratigraphy (Fig. 7). At the St. Stephens Quarry section, the position of the last occurrence of *T. cerroazulensis* and *Hantkenina* spp. has been in dispute for many years. Mancini (1979) observed that *T. cerroazulensis* extended up to the top of the Shubuta Clay. Several years later, Keller (1985) analyzed the same section and concluded that the last evolutionary occurrences of *T. cerroazulensis* and *Hantkenina* spp. occurred 12 ft below the Shubuta–Bumpnose boundary. She also concluded that the *T. cerroazulensis* and *Hantkenina* specimens in the upper Shubuta were reworked, based on their poor preservation and rare occurrence. Loutit et al. (1983) noted the occurrence of *T. cerroazulensis cocoaen-*

Table 8
Fossil events used in the composite section

No.	Species	c.u.	Event	No.	Species	c.u.	Event
73	*Pentadinium* sp. A	52	l.o.	29	*Hemiplacophora semilunifera*	102	l.o.
47	*Wetzeliella lobisca*	58	l.o.	36	*Cannosphaeropsis* sp. A	102	l.o.
82	*Polysphaeridium zoharyi*	59	f.o.	38	*Elytrocysta* sp. A of Head and Norris (1989)	103.5	l.o.
71	*Wetzeliella articulata*	62	l.o.	55	*Heteraulacacysta campanula*	105	f.o.
80	*Systematophora* sp. A	62	l.o.	14	*Charlesdowniea coleothrypta*	105	peak
73	*Pentadinium* sp. A	65	peak	26	*Cribroperidinium tenuitabulatum*	105	peak
58	*Wetzeliella symmetrica*	65	l.o.	44	*Systematophora placacantha*	105	peak
26	*Cribroperidinium tenuitabulatum*	67	l.o.	39	*Rhombodinium draco*	105	l.o.
55	*Heteraulacacysta campanula*	75	l.o.	42	*Batiacasphaera* aff. *baculata*	105	l.o.
11	*Cordosphaeridium cantharellum*	76	l.o.	46	*Enneadocysta multicornuta*	107	f.o.
75	*Impagidinium* sp. B	82	f.o.	47	*Wetzeliella lobisca*	107	f.o.
62	*Cordosphaeridium gracile*	84	l.o.	50	*Cordosphaeridium inodes*	107	f.o.
31	*Dinopterygium cladoides* sensu Morgenroth	85	l.o.	51	*Ascostomocystis potane*	107	f.o.
13	*Diphyes colligerum*	86.5	l.o.	52	*Homotryblium vallum*	107	f.o.
71	*Wetzeliella articulata*	93	f.o.	29	*Hemiplacophora semilunifera*	107	peak
9	*Operculodinium* aff. *centrocarpum*	94	peak	61	*Tectatodinium pellitum*	107.2	f.o.
67	*Operculodinium placitum*	94	peak	1	*Batiacasphaera compta*	107.2	l.o.
61	*Tectatodinium pellitum*	94	l.o.	24	*Batiacasphaera baculata*	108	l.o.
10	*Trigonopyxidia fiscellata*	95	l.o.	44	*Systematophora placacantha*	110	f.o.
65	*Cyclopsiella vieta*	96	f.o.	45	*Homotryblium plectilum*	111	f.o.
73	*Pentadinium* sp. A	96	f.o.	43	*Deflandrea heterophlycta*	113	f.o.
80	*Systematophora* sp. A	96	f.o.	49	*Enneadocysta arcuata*	113.5	f.o.
19	*Deflandrea phosphoritica*	96	peak	36	*Cannosphaeropsis* sp. A	115	f.o.
43	*Deflandrea heterophlycta*	97	peak	37	*Histiocysta* sp. A	115	f.o.
62	*Cordosphaeridium gracile*	98	f.o.	10	*Trigonopyxidia fiscellata*	115	peak
46	*Areosphaeridium multicornutum*	98	l.o.	16	*Lingulodinium pugiatum*	115	l.o.
68	*Apteodinium australiense*	100	f.o.	34	*Hystrichokolpoma globulum?*	115	l.o.
77	*Membranophoridium aspinatum*	100	f.o.	41	*Hystrichokolpoma cinctum*	115	l.o.
60	*Operculodinium divergens*	101	f.o.	66	*Nematosphaeropsis pusulosa*	115.5	f.o.
67	*Operculodinium placitum*	101	f.o.	24	*Batiacasphaera baculata*	117	f.o.
56	*Distatodinium* aff. *ellipticum*	102	f.o.	26	*Cribroperidinium tenuitabulatum*	117	f.o.
58	*Wetzeliella symmetrica*	102	f.o.	29	*Hemiplacophora semilunifera*	117	f.o.
59	*Glaphyrocysta* sp.	102	f.o.	31	*Dinopterygium cladoides* sensu Morgenroth	117	f.o.
98	*Heteraulacacysta leptalea*	102	f.o.	32	*Rottnestia borussica*	117	f.o.
15	*Muratodinium fimbriatum*	102	l.o.	39	*Rhombodinium draco*	117	f.o.

No. represents the taxon number used in the graphic correlation charts in Figs. 7 and 8; c.u. refers to composite unit, f.o. refers to first occurrence, l.o. refers to last occurrence, peak refers to high abundance levels of individual taxa. The Eocene–Oligocene boundary (33.7 Ma) occurs at a level of 99.5 composite units, Chron C13n–C12r magnetoboundary (33.05 Ma) corresponds to 53 c.u. Each c.u. has an equivalence of 0.014 Ma.

sis just below the top of the Shubuta Clay, whereas Pasley and Hazel (1990, 1995) identified the last occurrence of *Hantkenina alabamensis* 24 cm above the Shubuta–Bumpnose contact. Bybell and Poore (1983) also recovered some *Hantkenina* specimens from the upper Shubuta and Red Bluff Formations (at the Little Stave section in southern Alabama), which they interpreted as reworked specimens because they were filled with nannoplankton older than the sediment surrounding the foraminiferal test. A similar case has not been observed in the upper Shubuta at the St. Stephens Quarry section. Until further data prove that *T. cerroazulensis* and *Hantkenina* occurrences in the upper Shubuta Clay are reworked, we prefer to assume that those are true evolutionary occurrences. Therefore, the Eocene–Oligocene boundary is placed 24 cm above the Shubuta–Bumpnose contact in the St. Stephens Quarry sec-

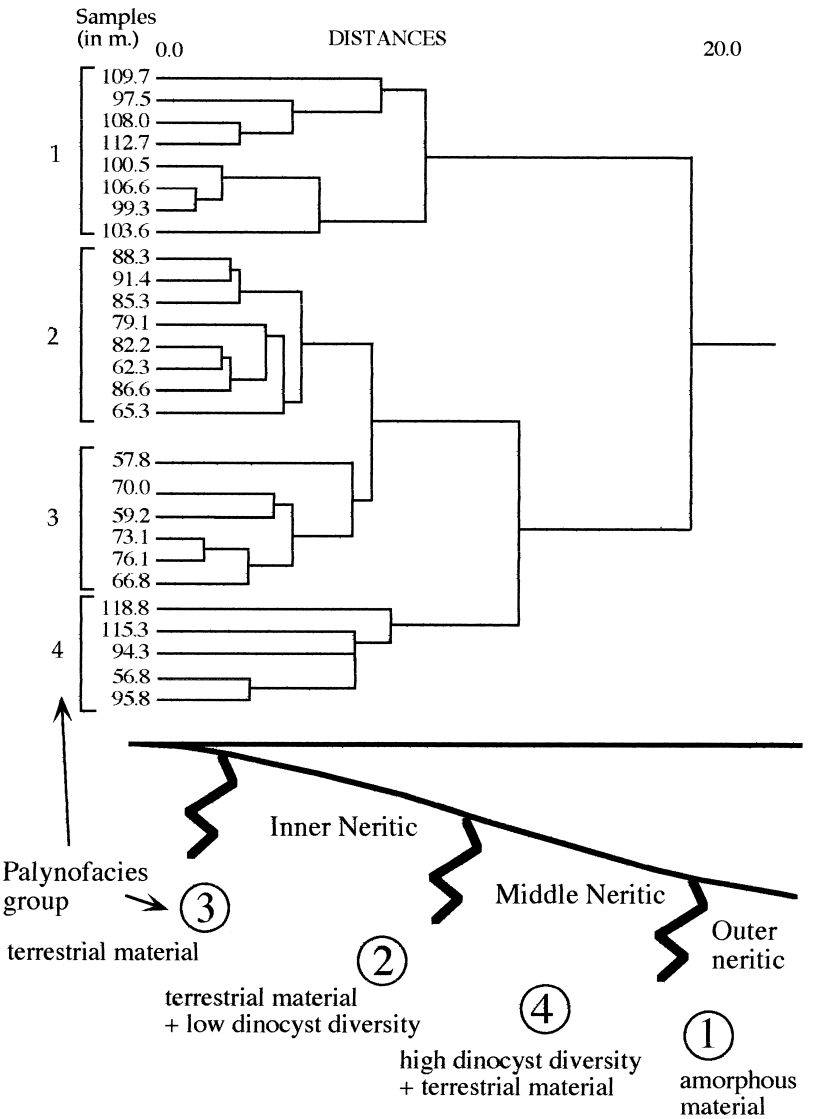

Fig. 5. Average linkage cluster analysis (with Euclidean distance) of dispersed organic matter in the #1 Young core. Each palynofacies group represents a group of samples with similar organic matter content, which accumulated in a similar position relative to the shoreline.

tion (last occurrence of *H. alabamensis*, Pasley and Hazel, 1990, 1995). The location of this boundary is reinforced by the C13n–C13r magnetoboundary, which is approximately 1.5 m above the Shubuta–Bumpnose contact in a core that was drilled 1.6 km from the St. Stephens Quarry section (Miller et al., 1993). This magnetoboundary is 14% older than the Eocene–Oligocene boundary (Berggren et al., 1995). The percentage refers to a fraction of the total duration of Chron C13r measured from the top down. This 14% would approximately coincide with the Shubuta–Bumpnose boundary. The only serious drawback with placing the Eocene–Oligocene at the base of the Bumpnose is the occurrence of *Cassigerinella chipolensis* in lower Shubuta samples (Miller et al., 1993). Although *Cassigerinella* has not been reported in Eocene sediments elsewhere, lower Shubuta samples have consistently yielded a

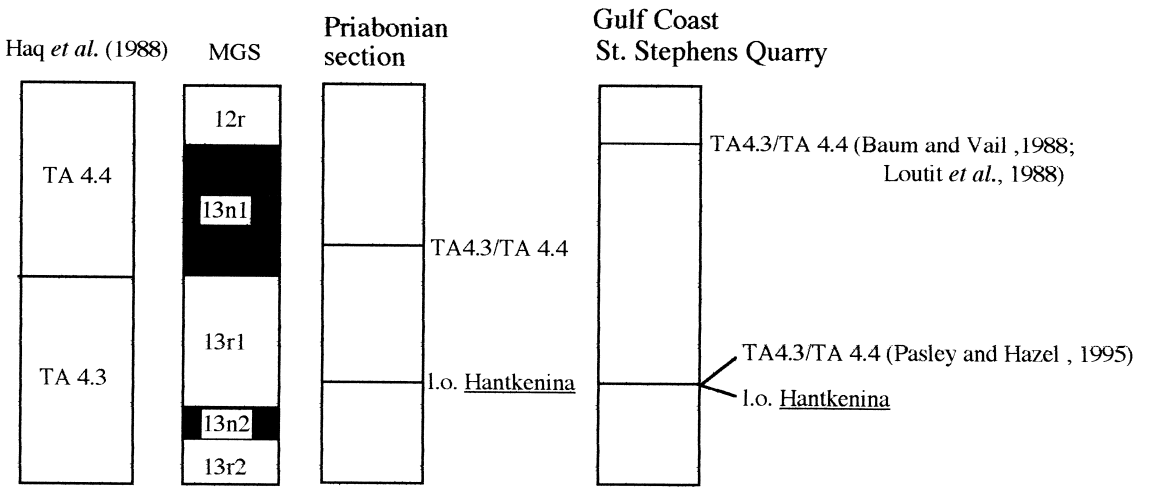

Fig. 6. Correlation of the Priabonian TA4.3/TA 4.4 sequence boundary with the Gulf Coast. Magnetostratigraphic (*MGS*) data after Miller et al. (1993) for the Gulf Coast. Location of the magnetoboundaries and the position of the last occurrence of *Hantkenina* in the Priabonian type-section were done by Brinkhuis and Visscher (1995) using correlation with dinoflagellates from the Massignano section.

robust P17 foraminifera assemblage (Mancini, 1979; Keller, 1985). Therefore, it is possible that the first evolutionary occurrence of *C. chipolensis* is latest Eocene.

The second datum used to tie the composite section to chronostratigraphy is the C13n–C12r Chron magnetoboundary (Miller et al., 1993) at the Forest Hill–Mint Spring contact in the St. Stephens Quarry section. This magnetoboundary is dated as 33.05 Ma (Berggren et al., 1995).

A third datum, which was also used to test the validity of our composite section, is the last occurrence of *Hantkenina alabamensis* in the R2089 Type Red Bluff section (or Chicasawhay River section of Pasley and Hazel, 1995). This datum occurs 0.1 m above the Shubuta–Red Bluff contact (Pasley and Hazel, 1995).

These three datums were projected onto the correlation line drawn by the comparison of the composite section with the St. Stephens Quarry and R2089 sections (Fig. 7). The line of correlation for the St. Stephens Quarry section indicates an interval of 80 cm of extreme condensation, lasting about 13.7 composite units (i.e., 0.191 Ma) (Fig. 7). This condensed interval starts 20 cm below the Shubuta–Bumpnose contact and ends 60 cm above it. The identification of the condensed interval is based on the first and last occurrence datums used in the correlation. Several events which are not coeval appear together in the same sample. For example, the following events are recorded in sample 4.7 m (refer to Figs. 7 and 15 for sample position): abundance peak of *Hemiplacophora semilunifera* (#29 taxon), first occurrence (f.o.) of *Wetzeliella lobisca* (#47), last occurrence (l.o.) of *Elytrocysta* sp. A (#38), l.o. of *Hemiplacophora semilunifera* (#29) and f.o. of *Operculodinium placitum* (#67). However, these events occur at different levels in the standard composite section (Table 8), indicating that the dinocyst assemblage in the sample is the result of extremely slow sedimentation. A similar case can be made for sample 5.0 m: f.o. of *Ascostomocystis potane* (#51), *Operculodinium divergens* (#60), and *Membranophoridium aspinatum* (#77), peak of *Deflandrea heterophlycta* (#43), f.o. of *Cyclopsiella vieta* (#65), l.o. of *Tectatodinium pellitum* (#61), and peak of *Operculodinium placitum* (#67). Sample 5.3 m has a similar assemblage to sample 5.0 m but it does not show up in the correlation, because all of the first occurrence datums were already recorded in sample 5.0 m. Furthermore, Loutit et al. (1988) interpreted the first 60 cm of the Bumpnose (or unnamed blue clay) as a condensed section, based on gamma ray log and foraminifera. The last occurrence of *H. alabamensis*, at 24 cm above the base of the Bumpnose, lies in the middle of this condensed section. To extrapolate

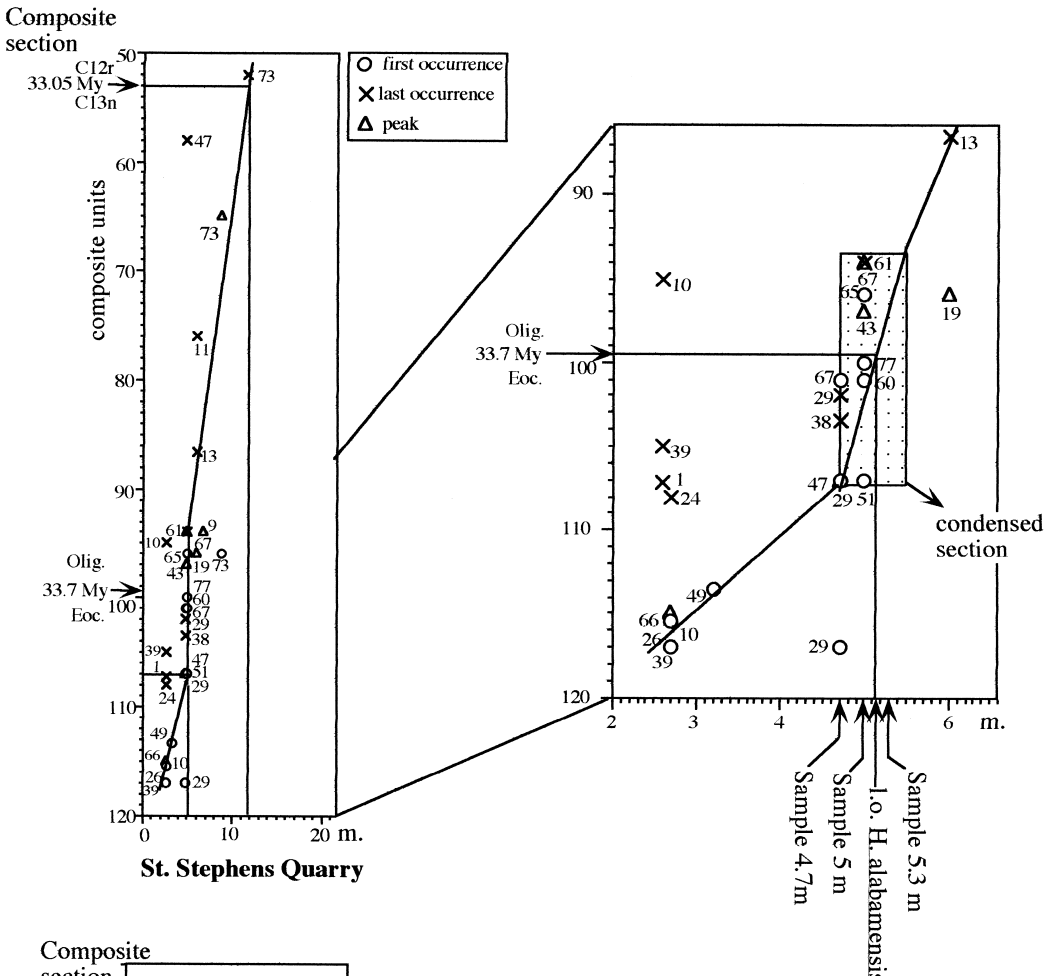
Composite section
C12r
33.05 My
C13n
composite units
first occurrence
last occurrence
peak
Olig.
33.7 My
Eoc.
condensed section
Sample 4.7m
Sample 5 m
l.o. H. alabamensis
Sample 5.3 m
m.
St. Stephens Quarry

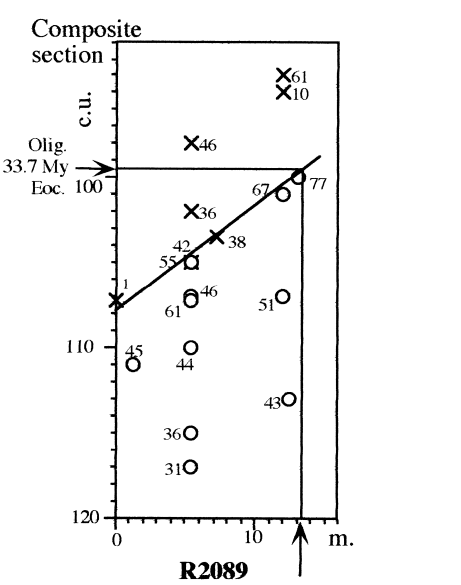
Composite section
c.u.
Olig.
33.7 My
Eoc.
m.
R2089
l.o. H. alabamensis

this datum onto the composite section, we delimited the ranges of the condensed section and established an average rate of accumulation for the condensed section (Fig. 7). Subsequently, the *H. alabamensis* datum was projected onto the average accumulation rate and from there onto the composite section. A level at 99.5 composite units was found in the composite section. To test this result, the *H. alabamensis* datum of the R2089 section was projected onto the correlation line and from there onto the composite section (Fig. 7). The result was identical to that of the St. Stephens Quarry section, and the Eocene–Oligocene boundary was placed at 99.5 composite units.

The C13n–C12r magnetoboundary (33.05 Ma) at the St. Stephens Quarry section occurred at the composite units 53 when projected onto the composite section (Fig. 7). The composite section was also compared with the other three sections studied (#1 Young, #1 Wayne, and #1 Ketler; Fig. 8). A duration of 0.014 Ma per composite unit was calculated from the age-data points used for correlation.

6. Dinocyst paleoecology

Some extant dinoflagellate cysts are sensitive environmental indicators, and are therefore of potential use in paleopalynology. Several studies (e.g., Wall et al., 1977; Dale, 1996) have indicated that four types of environmental signals can be deduced from Recent cyst distributions: (1) surface water temperature, (2) a coastal/oceanic signal, (3) a salinity signal, and (4) a productivity signal. Wall et al. (1977) and Dale (1996) identified a nearshore–offshore trend, based on the presence or absence of oceanic dinocyst species (which reaches a maximum abundance in the middle of the ocean), and on proportional changes in species composition from nearshore to offshore. Cyst data also suggested a broad salinity control on distribution, indicating three zones, namely freshwater, brackish, and normal salinity waters (>27‰). By far the highest number of cysts are from coastal/neritic species living in waters with salinities ranging from estuarine (20‰) to marine (35‰, euryhaline). The end members (freshwater/brackish and fully oceanic) are also distinctive. Cyst analyses can also assist in identifying paleoproductivity (mainly coastal upwelling and eutrophication) (Dale, 1996). In summary, water mass types combined with hydrodynamic systems are the most important factors controlling cyst distribution in the bottom thanatocoenosis of today's oceans (Wall et al., 1977). Given these facts, the distribution patterns of dinoflagellate cysts in the fossil record can be used to infer variations in water masses, which in turn can be related to changes in relative sea level (nearshore–offshore signal), sea surface temperature, salinity, and water productivity. This approach has been used by several authors, such as Châteauneuf (1983), Köthe (1990), Brinkhuis (1992, 1994), Brinkhuis and Biffi (1993) and Zevenboom et al. (1994). However, it is important to keep in mind that cyst thanatocoenosis may not always correspond to theca biocoenosis. The dinocyst record can be a mixture of cysts transported by currents and cysts derived from theca living in the water mass above the bottom where the cysts are finally accumulated.

Relative sea level fluctuations in neritic settings are usually reflected in varying abundances of taxa, which typically occur in restricted marine or inner neritic water masses versus those that characteristically occur in outer neritic waters (Brinkhuis, 1994, p. 142). In order to determine where dinocyst taxa occur along an onshore–offshore transect, we used two techniques: (1) detailed literature research focusing on paleoenvironmental interpretations for the dinocysts found in this study (Appendix A); and (2) multivariate analysis of the dinocyst distribution. The use of multivariate statistical techniques relies on the basic assumption that dinocysts co-occurring in the same samples lived in similar environments, and that statistical parameters evaluate how strong a given co-occurrence is. This approach allowed us to test previous hypotheses on specific dinocyst paleoenvironments, in addition to providing more hypothesis

Fig. 7. Line of correlation of St. Stephens Quarry and R2089 Type Red Bluff sections versus the composite section. See Table 8 for the names of taxa used for graphic correlation, and Section 5 on how the positions of the Eocene–Oligocene boundary were derived in the sections.

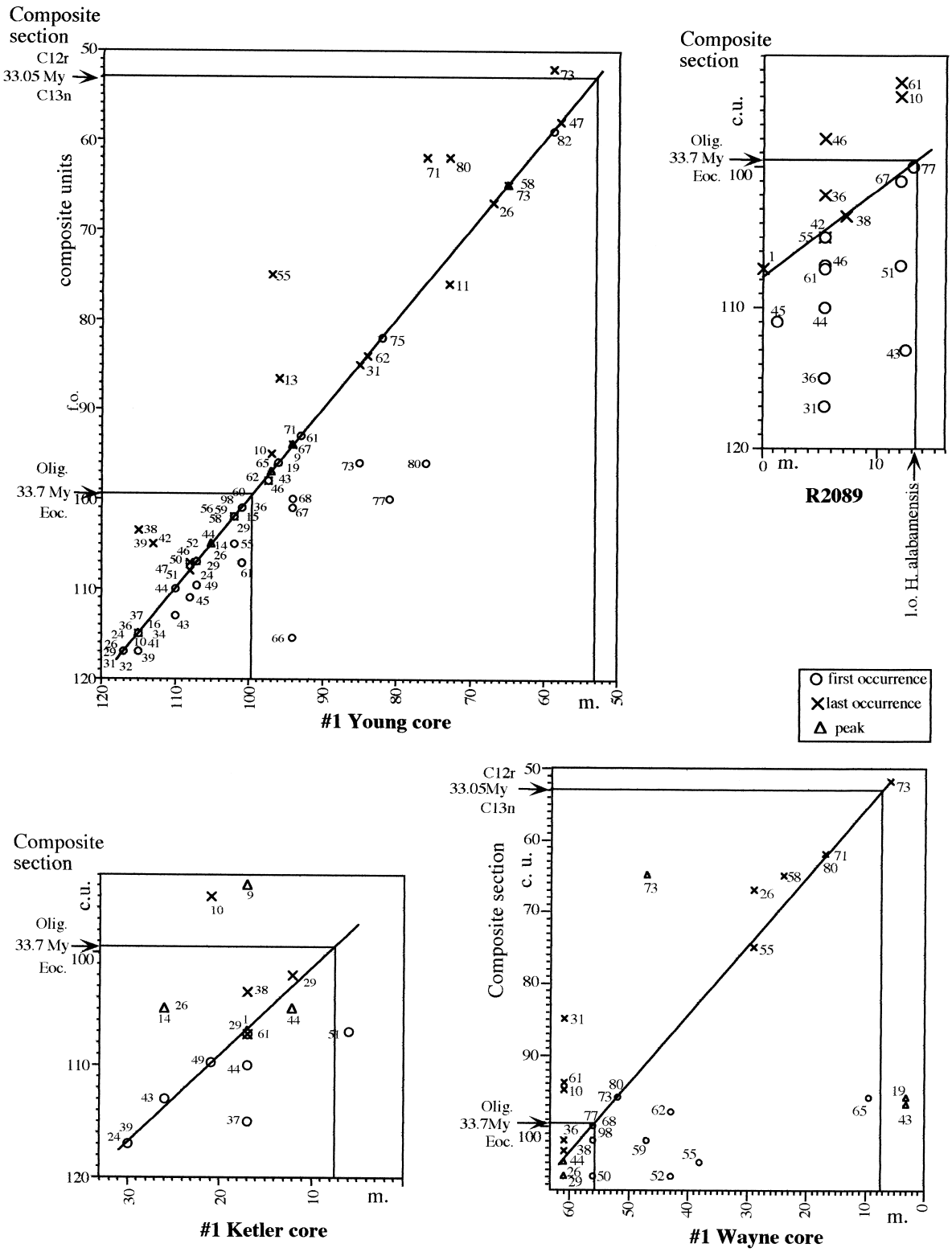
Composite section
C12r
33.05 My
C13n
composite units
f.o.
Olig.
33.7 My
Eoc.
m.
#1 Young core
Composite section
c.u.
Olig.
33.7 My
Eoc.
R2089
l.o. H. alabamensis
first occurrence
last occurrence
peak
Composite section
c.u.
Olig.
33.7 My
Eoc.
#1 Ketler core
C12r
33.05My
C13n
Composite section
c. u.
Olig.
33.7My
Eoc.
#1 Wayne core

on dinocyst–environment relationships which can be tested in future studies.

The choice of which multivariate analysis to perform on any data set depends on the structure and noisiness of the data, the specific question being addressed, and the philosophy behind the study (Kovach, 1989). While considering a problem similar to the one being addressed in this study, Kovach (1989) analyzed a noisy and non-normal data set, with a view to relating species distribution to a terrestrial–marginal marine gradient, as well as inferring what groups characterized each environment. He found that the best method (which provides an unambiguous answer to the question; Pielou, 1984) was the Spearman rank-order coefficient performing a non-metric multidimensional scaling (MDS) analysis. MDS identifies the major terrestrial–marginal marine gradient along the first and second axes, and seems to be least vulnerable to distortion from high data diversity, non-normality, and non-linearity. In this study, MDS analysis was performed on a subset of data from the original distribution range charts. Dinocysts with high abundances and those with recognized paleoenvironmental significance were selected for the analysis. Thus, a set of 32 dinocysts were used for the MDS analysis, the result of which is illustrated in Fig. 9.

The interpretation of the MDS analysis was done primarily on the basis of the spatial position of each taxon along the first and second order axes, and on literature review. Our main goal was to identify nearshore–offshore trends, if present. Information on sea surface temperature preferences for the recorded dinocysts is so scarce that no attempt has been made to infer a sea surface temperature signal, although it may be present. Seven dinocysts groups were identified, and five of them are interpreted as representing an inshore–offshore trend (Fig. 9). The environmental interpretations (e.g., inner, middle, outer neritic) are used in a relative sense rather than in an absolute one. These terms only represent the position of a dinocyst assemblage relative to another one rather than an absolute position along the shelf or an absolute water depth. Variations in the relative proportions of those groups through time are interpreted here to represent variations in the type of water mass, which in turn is linked to relative variations in sea level and/or run-off changes. The paleoecological groups, characteristic dinocysts and other marine palynomorphs (Appendix A) are discussed in the paragraphs below.

Group A: *Homotryblium plectilum* and *Pediastrum* (an alga). This group is interpreted here as representing innermost neritic settings. *Homotryblium* has been reported as a marginal marine taxon by Zevenboom et al. (1994), Brinkhuis (1994), and Dale (1996). *Pediastrum* is more abundant in estuarine environments than in neritic ones (Brown and Downie, 1984).

Group B: *Ascostomocystis potane* (an acritarch) and *Glaphyrocysta* sp. The maximum abundance of this group indicates inner neritic settings. Brinkhuis (1994) identified a higher abundance of *Ascostomocystis* in inner neritic environments. *Glaphyrocysta* was suggested as (open marine) inner neritic by Brinkhuis and Zachariasse (1988), Brinkhuis (1994) and Powell et al. (1996).

Group C: *Cordosphaeridium* spp., *Cleistosphaeridium* sp., *Systematophora placacantha*, *Enneadocysta* spp., *Operculodinium* aff. *centrocarpum*, *Lingulodinium* spp., *Achomosphaera alcicornu*, *Spiniferites pseudofurcatus*, *Spiniferites ramosus*, and *Pentadinium laticinctum*. In general, these taxa are abundant in neritic settings (either inner, middle or outer). *Cordosphaeridium* indicates open sea conditions (Downie et al., 1971; Islam, 1984; Köthe, 1990). Normal marine, shallow water was suggested for *Cleistosphaeridium* (Köthe, 1990). *Systematophora placacantha* indicates open marine water masses (Köthe, 1990). *Enneadocysta pectiniformis* and allied taxa were interpreted as neritic by Brinkhuis (1994). *Operculodinium* suggests neritic conditions (Brinkhuis et al., 1992), and *O. centrocarpum* is also indicative of the shelf (Wall et al., 1977; Brown and Downie, 1984; Brinkhuis, 1994). *Achomosphaera alcicornu* is more abundant

Fig. 8. Line of correlation for the #1 Young, #1 Wayne and #1 Ketler cores, and R2089 Type Red Bluff section versus the composite section. See Table 8 for the names of taxa used for graphic correlation, and Section 5 on how the positions of the Eocene–Oligocene boundary were derived in the sections.

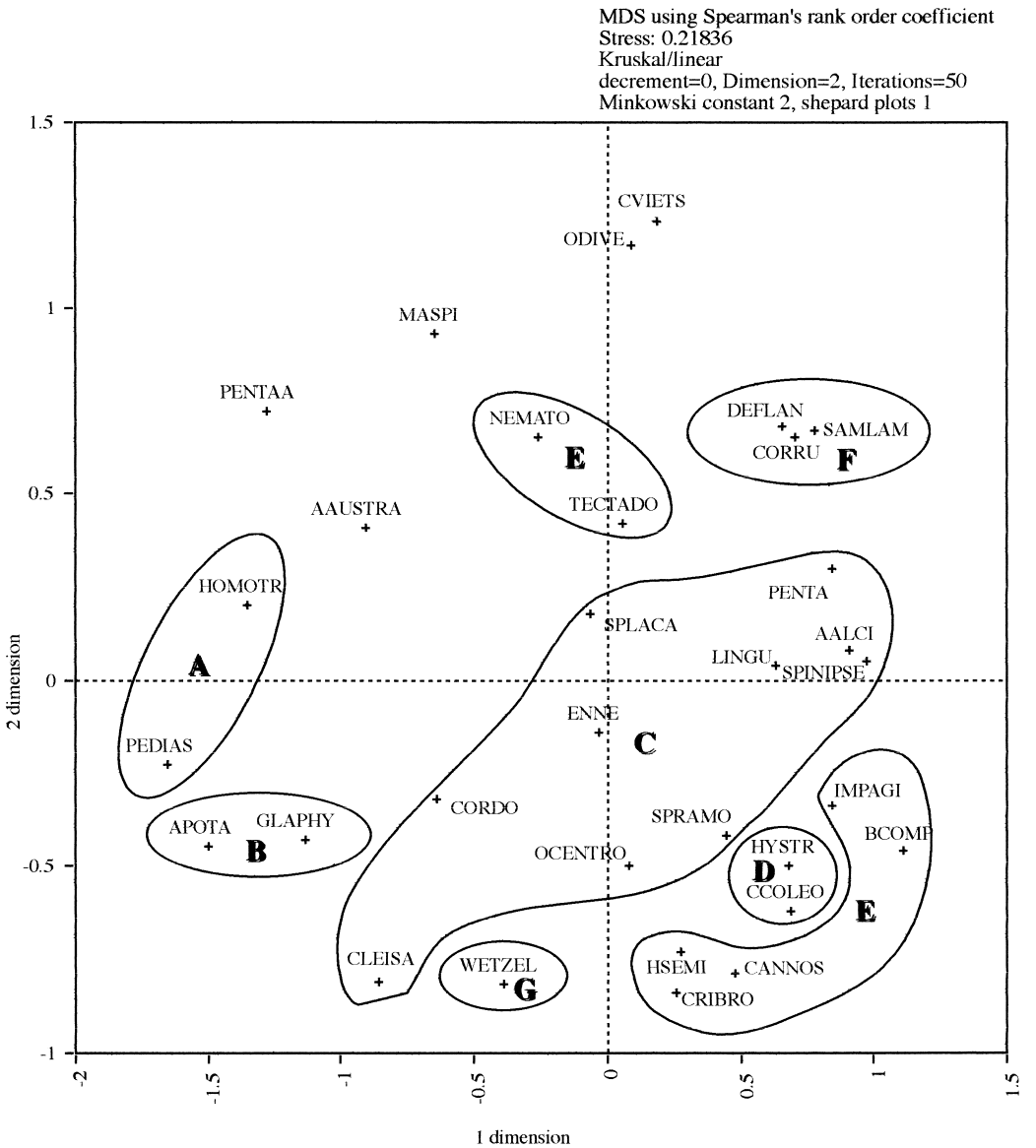

Fig. 9. Scattergram of species ordinations, from a non-metric multidimensional scaling (*MDS*) analysis using Spearman's rank-order coefficient. See discussion about the seven dinocyst groups identified. Species designations are as follows: *Achomosphaera alcicornu* AALCI, *Apteodinium australiense* AAUSTRA, *Ascostomocystis potane* (an acritarch) APOTA, *Batiacasphaera compta* BCOMP, *Cannosphaeropsis* sp. A CANNOS, *Charlesdowniea coleothrypta* CCOLEO, *Cleistosphaeridium* sp. CLEISA, *Cordosphaeridium* spp. CORDO, *Corrudinium incompositum* CORRU, *Cribroperidinium tenuitabulatum* CRIBRO, *Cyclopsiella vieta* (an acritarch) CVIETS, *Deflandrea* spp. DEFLAN, *Enneadocysta* spp. + *Areosphaeridium* spp. ENNE, *Glaphyrocysta* sp. GLAPHY, *Hemiplacophora semilunifera* HSEMI, *Homotryblium plectilum* HOMOTR, *Hystrichokolpoma rigaudiae* HYSTR, *Impagidinium dispertitum*, IMPAGI, *Lingulodinium* spp. LINGU, *Membranophoridium aspinatum* MASPI, *Nematosphaeropsis pusulosa* NEMATO, *Operculodinium* aff. *centrocarpum* OCENTRO, *Operculodinium divergens* ODIV, *Pediastrum* (an alga) PEDIAS, *Pentadinium laticinctum* PENTA, *Pentadinium* sp. A PENTAA, *Samlandia clamydophora* SAMLAM, *Spiniferites pseudofurcatus* SPINIPSE, *Spiniferites ramosus* SPRAMO, *Systematophora placacantha* SPLACA, *Tectatodinium pellitum* TECTADO, *Wetzeliella* spp. WETZEL.

in open sea (Downie et al., 1971) and *Achomosphaera* in neritic environments have been reported by Brinkhuis and Zachariasse (1988), Brinkhuis et al. (1992) and Brinkhuis (1994). *Spiniferites* spp. are indicative of neritic open marine (Downie et al., 1971; Islam, 1984; Brinkhuis, 1994), with *S. ramosus* (Wall et al., 1977; Harland, 1983; Wrenn and Kokinos, 1986) and *S. pseudofurcatus* being reported as neritic dwellers (Brinkhuis, 1994). *Lingulodinium* suggests euryhaline (Islam, 1984), nearshore conditions (Brinkhuis et al., 1992).

Group D: *Hystrichokolpoma rigaudiae* and *Charlesdowniea coleothrypta*. This group is tentatively interpreted as middle neritic by cluster position. These taxa are grouped separately because they cluster apart from group C and are closer to group E which is outer neritic to oceanic. Also they form a distinct group in a separate analysis using unweighted pair group average linkage cluster analysis with Spearman coefficient of similarity (figure is not shown in this study). The fact that these two species grouped together was previously indicated by Goodman (1979), using a chi-square index applied to presence–absence data, and a Jaccard coefficient of similarity (of 33, range 0–100). Goodman (1979), however, classified them into two separate groups: *C. coleothrypta* as being more offshore and *H. rigaudiae* as being more inshore. Surprisingly, *Charlesdowniea coleothrypta* was not clustered with any *Wetzeliella*, as obtained by the multivariate analysis of Goodman (1979). Data from the London Clay of the Hampshire and London basins indicate that *Charlesdowniea* is more abundant than *Wetzeliella* in offshore parts of the basins (Graham Williams, pers. commun., 1998).

Group E: *Cribroperidinium tenuitabulatum*, *Cannosphaeropsis* sp. A, *Impagidinium dispertitum*, *Batiacasphaera compta*, *Hemiplacophora semilunifera*, *Nematosphaeropsis pusulosa* and *Tectatodinium pellitum*. The last two taxa occur in a group separated from the first five taxa (Fig. 9), but are included here because *Nematosphaeropsis* is a recognized outer neritic to oceanic taxon (Dale, 1996) or oceanic taxon (Brinkhuis et al., 1992; Brinkhuis and Biffi, 1993; Zevenboom et al., 1994). *Tectatodinium pellitum* is also more common in outer shelf and slope rise (Wall et al., 1977). Both taxa are probably not clustered with the other five taxa because another environmental variable, besides inshore–offshore trend, is probably controlling their distribution. This other variable could be warmer sea water since *T. pellitum* is considered a warm water taxon (Head, 1994). *Impagidinium* is a recognized outer neritic–oceanic taxon (Wrenn and Kokinos, 1986; Edwards and Andrle, 1992; Mudie and Harland, 1996) or oceanic taxon (Harland, 1983; Brinkhuis et al., 1992; Brinkhuis and Biffi, 1993; Zevenboom et al., 1994; Dale, 1996). While analyzing sea level changes in NW Tunisia, Brinkhuis and Zachariasse (1988) interpreted an interval (named I) characterized by a high *Batiacasphaera* content and up to 10% *Impagidinium*, which they interpreted as a more offshore environment than intervals II and III. *Cannosphaeropsis* is recognized as oceanic (Brinkhuis and Biffi, 1993), with *Cribroperidinium tenuitabulatum* indicating deep and cool water conditions. *Hemiplacophora semilunifera* has been reported as being indicative of outer neritic environments (Brinkhuis, 1994).

Group F: *Deflandrea* spp., *Corrudinium incompositum*, and *Samlandia clamydophora*. *Deflandrea* is a widely recognized cyst from a heterotrophic dinoflagellate which thrives in high-nutrient settings (Brinkhuis et al., 1992; Brinkhuis, 1994). The close clustering of the other two taxa suggests that they may be important in this type of environment.

Group G: *Wetzeliella* spp. No clear interpretation is given for this genus. It is isolated in the analysis, indicating that it probably lived in restricted conditions which constrained its co-occurrence with other dinoflagellates. Lagoonal, estuarine and brackish environments have been indicated as ecological habitats for the genus (Downie et al., 1971; Islam, 1984; Köthe, 1990). Its abundance, however, was never dominant (never more than 5%) in any of the studied samples.

Three relative paleobathymetric curves were plotted for each stratigraphic section. The first one is a weighted mean ($\sum n_i(i)/n$) of the innermost, inner, middle, and outer neritic to oceanic groups identified in the MDS analysis, where n represents the total number of taxa (abundance) in a particular sample and n_i represents the abundance of each ecological group; (i) represents pre-established categories whereby innermost neritic, inner neritic, middle and outer neritic–oceanic groups are weighted 1, 2, 3,

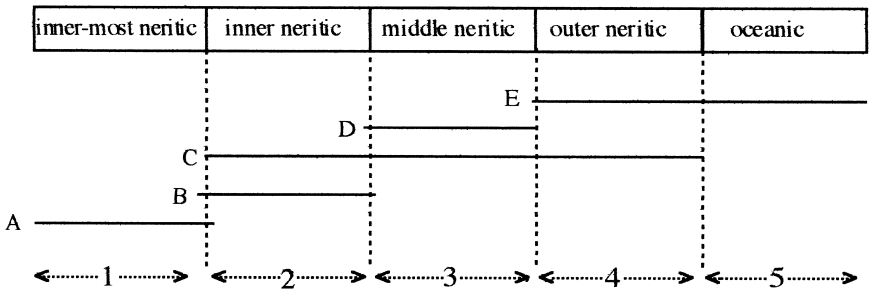

$$DPI = \frac{A*1+B*2+((C*2+C*3+C*4)/3)+D*3+((E*4+E*5)/2)}{A+B+C+D+E}$$

Fig. 10. Dinocyst paleobathymetric index (*DPI*). The value produced by the weighted mean (herein called DPI) combines all the information given by the dinocysts in a sample. Plotting this value through the section can provide us with general trends in changes of depositional environments through time.

and 4, respectively (Fig. 10). Since dinoflagellate cyst distribution is controlled by the type of water mass and hydrodynamic factors, a particular sample can contain a dinocyst assemblage composed of dinoflagellates which lived in the overlying water mass, plus a set of cysts transported from different areas by currents. The value produced by the weighted mean (here called dinocyst paleobathymetric index, DPI) combines all the information given by the dinocysts of a sample in a meaningful value, which represent the average given by the whole assemblage. Plotting this value through the section can provide us with general trends in changes of depositional environments through time (Figs. 11–15).

The second curve plotted in Figs. 11–15 was the abundance of the *Deflandrea* group. Increased nutrient availability can occur as a result of the introduction of shelf-stored nutrients in the photic zone through turbulent mixing associated with flooding events (Brinkhuis, 1994). Other factors, such as changes in run-off in river mouths, upwelling and deep mixing, also increase nutrient availability (Brinkhuis, 1994).

The third curve consists of an abundance of reworked dinocysts. Higher abundances of reworked material may be expected during highstand and lowstand systems tracts because clast input from the continent is higher. The status of 'reworked' for a dinocyst was to establish on the following basis: (a) if it has not been reported for the Tertiary (e.g., *Alisogymnium*, *Dinogymnium*, *Odontochitina*); and (b) if it has a Paleogene record but it became extinct before the latest Eocene in the Gulf Coast (e.g., *Lentinia* sp., Lucy Edwards, pers. commun., 1995).

7. Sequence stratigraphic interpretation

7.1. #1 Young

The dating of the #1 Young core was done by comparing the section with the standard composite section produced in this study (Fig. 8). The Eocene–Oligocene boundary is located at 99.5 m, 2.3 m below the Shubuta Clay–Red Bluff boundary. Based on the paleobathymetric curves reconstructed from palynofacies and dinocyst paleoecology, two important flooding surfaces were identified (Fig. 11). The first flooding surface occurs at 107.5 m (353 ft), 10.3 m below the Shubuta Clay–Red Bluff boundary, while the other surface is identified at 57.7 m (189.4 ft) at the Forest Hill–Mint Spring contact. The horizon at 107.5 m is considered a maximum flooding surface because of the following reasons: (a) it is a green calcareous claystone with abundant uvigerinids, which are deep water benthic foraminifera (Dockery et al.,

Fig. 11. Sequence stratigraphic interpretation for the #1 Young core. Refer to Figs. 4 and 5 for the derivation of paleobathymetric curve from palynofacies data, and Fig. 9 for taxa used in calculating the dinocyst paleobathymetric index.

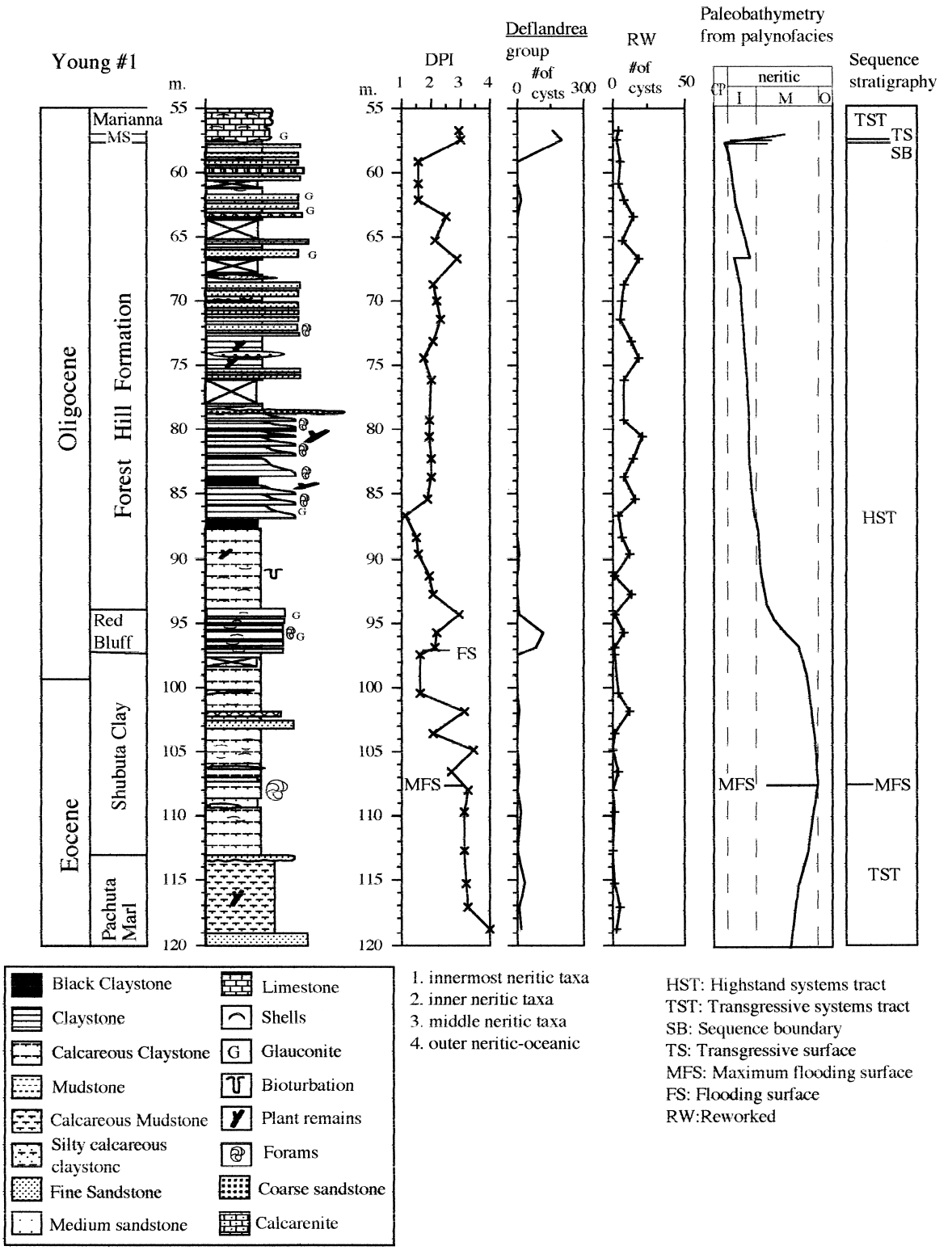
Young #1
m.
Marianna
MS
Oligocene
Forest Hill Formation
Red Bluff
Eocene
Shubuta Clay
Pachuta Marl
DPI
1 2 3 4
Deflandrea group
#of cysts
0 300
RW
#of cysts
0 50
Paleobathymetry from palynofacies
neritic
CP I M O
Sequence stratigraphy
TST
TS
SB
HST
MFS
TST
FS
Black Claystone
Claystone
Calcareous Claystone
Mudstone
Calcareous Mudstone
Silty calcareous claystone
Fine Sandstone
Medium sandstone
Limestone
Shells
Glauconite
Bioturbation
Plant remains
Forams
Coarse sandstone
Calcarenite
1. innermost neritic taxa
2. inner neritic taxa
3. middle neritic taxa
4. outer neritic-oceanic
HST: Highstand systems tract
TST: Transgressive systems tract
SB: Sequence boundary
TS: Transgressive surface
MFS: Maximum flooding surface
FS: Flooding surface
RW:Reworked

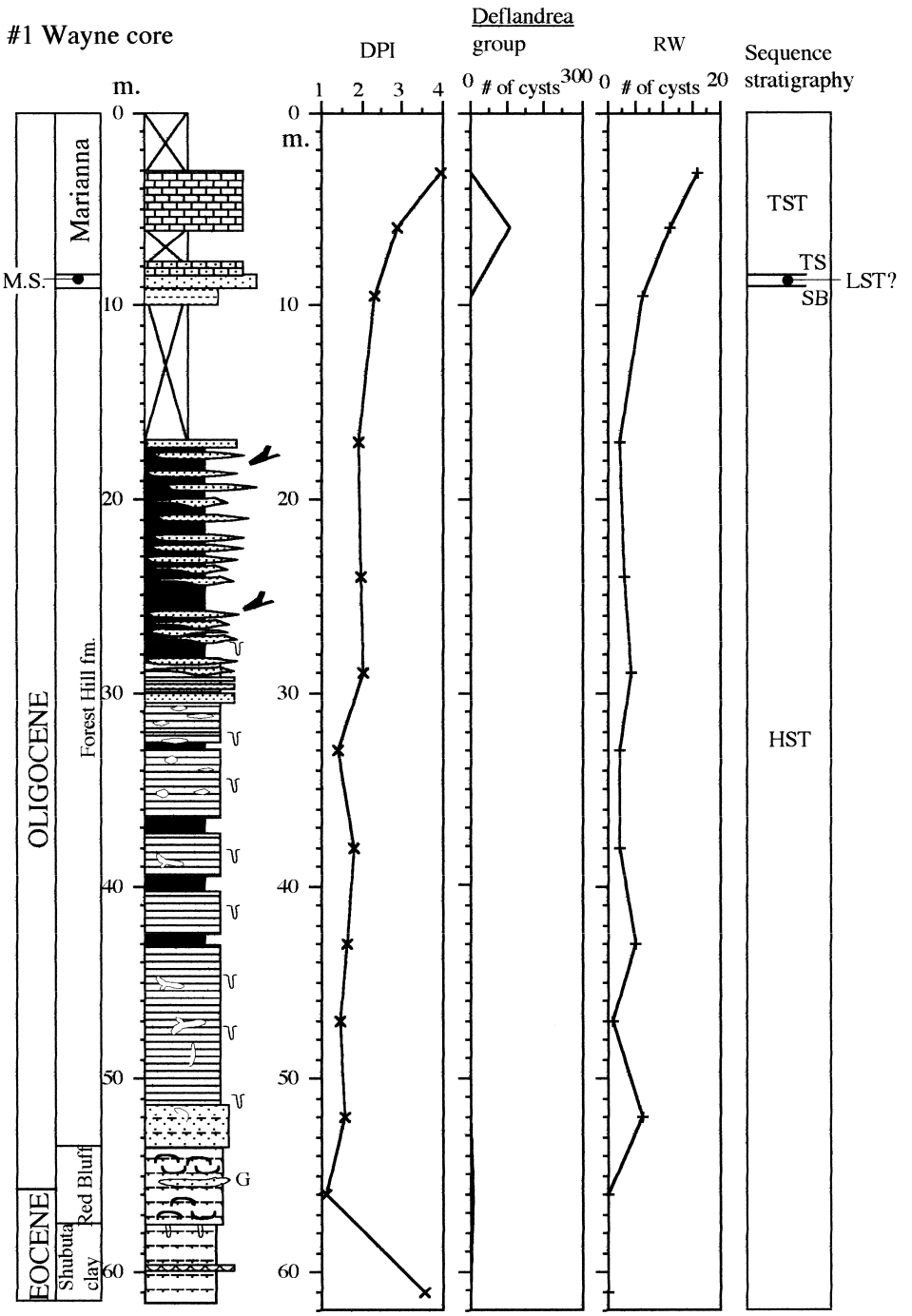

Fig. 12. Sequence stratigraphic interpretation for the #1 Wayne core. Refer to Fig. 9 for taxa used in calculating the dinocyst paleobathymetric index, and Fig. 11 for the key to lithologic symbols.

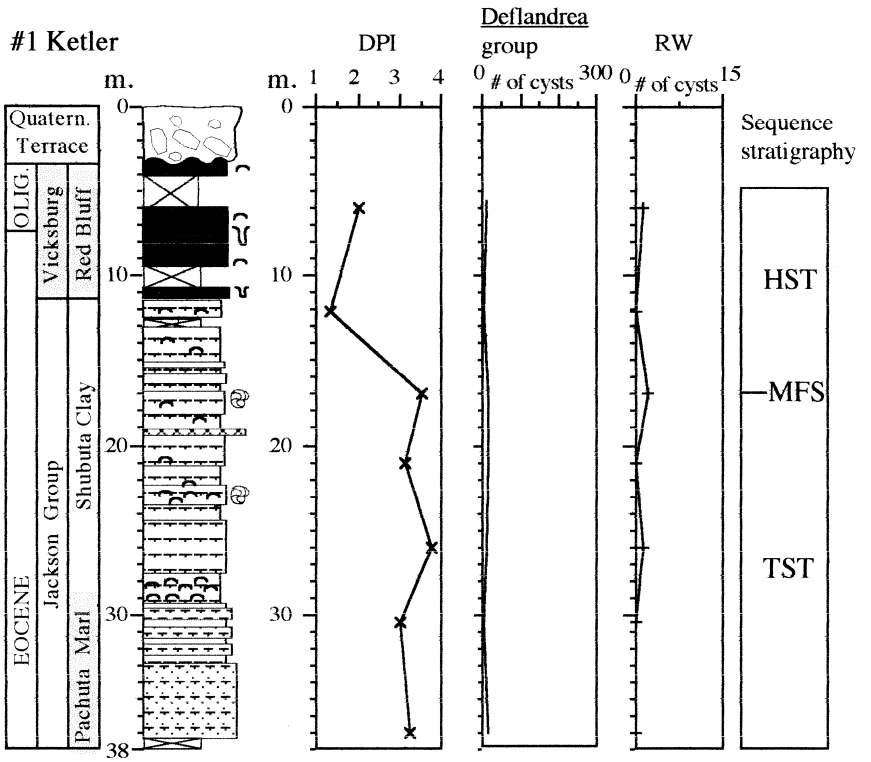

Fig. 13. Sequence stratigraphic interpretation for the #1 Ketler core. Refer to Fig. 9 for taxa used in calculating the dinocyst paleobathymetric index, and Fig. 11 for the key to lithologic symbols.

1994); (b) it occurs between two of the samples with the highest concentration of marine-derived organic matter (amorphous and dinocysts, Table 2, Fig. 4). This level also corresponds to a high value (3.2) in the dinocyst paleobathymetric index (Fig. 11), and is 0.9 m above a gamma ray peak (Fig. 4). This maximum flooding surface is eight composite units (0.112 Ma) older than the Eocene–Oligocene boundary. A minor flooding surface is identified at the Shubuta–Red Bluff contact at 97.2 m (319 ft), based on the lithological change (olive-gray clay to gray, fossiliferous, glauconitic mudstone) and an increase in abundance of the *Deflandrea* group.

The second major flooding event is identified at the Forest Hill–Mint Spring contact at 57.72 m (33.1 Ma). We believe that in this case, a sequence boundary coincides with a transgressive surface (Fig. 11). Although an abrupt landward shift in facies, which would be indicative of a sequence boundary, was not detected at the contact, several lines of evidence suggest this hypothesis. The contact is sharp, irregular, and marked by an abraded shell lag and rounded intraclasts. Furthermore, the upper facies of the Forest Hill indicate a fast net progradation of the shoreline, suggesting that space of accommodation was rapidly decreasing, which is typical of the youngest parts of highstand deposits. If this section is located in a bypass zone during a relative sea level fall, the sequence boundary would be impossible to detect on the basis of palynofacies and paleoecology alone. This hypothesis can be confirmed in up-dip and down-dip sections if forced regressions or incised valleys are found (Posamentier et al., 1992). If the proposed lowstand deposit in the #1 Wayne core (see discussion below) above the sequence boundary at the Forest Hill–Mint Spring contact is proven, it would confirm the nature of this boundary.

The Pachuta Marl and lower Shubuta Clay constitute a transgressive systems tract. The lower Pachuta is characterized by calcareous mudstones which

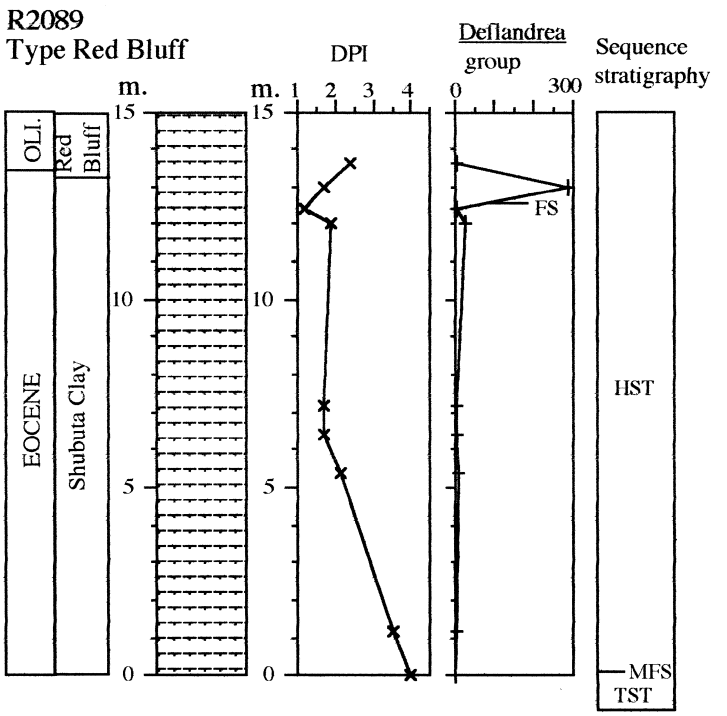

Fig. 14. Sequence stratigraphic interpretation and graphic correlation for the R2089 section. Refer to Fig. 9 for taxa used in calculating the dinocyst paleobathymetric index, and Fig. 11 for the key to lithologic symbols.

change gradationally to calcareous claystones in the lower Shubuta. The upper Shubuta, Red Bluff, and Forest Hill Formations correspond to a highstand systems tract. There is an increase in the amount of reworked dinocysts and the facies change gradationally from calcareous claystones in the upper Shubuta to dark gray carbonaceous claystones, which intercalate with fine quartz arenites toward the top of the Forest Hill (Fig. 11). This facies change is indicative of a net progradation of the paleoshoreline. A lowstand was not detected in the core. The Mint Spring Marl and lower Marianna Limestone constitute a transgressive systems tract, and the dominance of limestone suggests a net decrease in the terrigenous supply to the basin.

7.2. #1 Wayne

The Eocene–Oligocene boundary is present at 55.7 m, 1.9 m above the Shubuta–Red Bluff contact (Fig. 8). The Chron 13n–C12r boundary occurs at 7.1 m, 2 m above the Forest Hill–Mint Spring contact. A sequence boundary is interpreted at the Forest Hill–Mint Spring contact, where the contact is sharp, irregular and burrowed, and with a pavement of intraclasts (clay clasts). The lithofacies below the contact consists of a brown carbonaceous mudstone while above it is a 60-cm-thick, white medium-grained quartz sandstone with calcareous cement (the Mint Spring) (Fig. 12). Although samples from this sandstone interval were not analyzed, the unit is interpreted as a deposit of a possible lowstand systems tract on the basis of lithological characteristics. This sandstone probably represents part of a forced regression deposit, although the lateral continuity of the sand body is uncertain. The Mint Spring sandstone is overlain by a gray porous limestone which corresponds to the lower Marianna Limestone. The Mint Spring–Marianna contact is sharp and is interpreted as a transgressive surface. The paleobathymetric data, including an increase in the *Deflandrea* group, indicate a deepening across this interval.

The upper Shubuta, Red Bluff, and Forest Hill

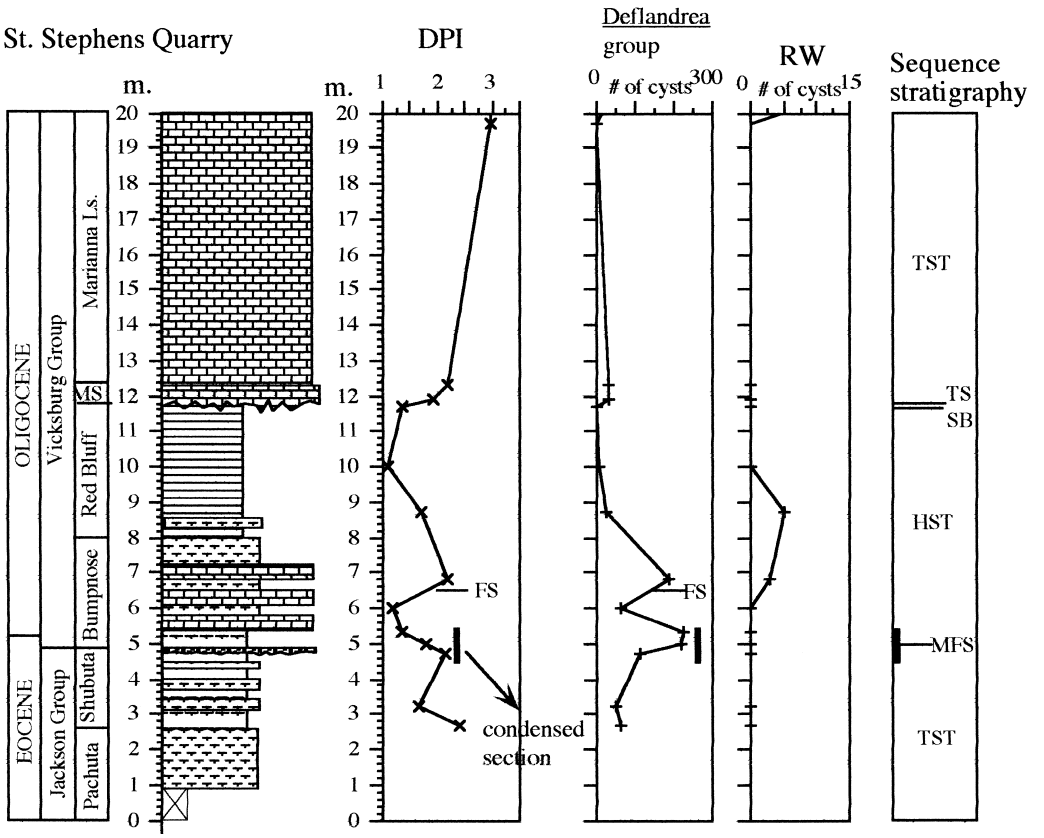

Fig. 15. Sequence stratigraphic interpretation for the St. Stephens Quarry section. Refer to Fig. 9 for taxa used in calculating the dinocyst paleobathymetric index, and Fig. 11 for the key to lithologic symbols. An 80-cm-condensed section containing the maximum flooding surface and the Eocene–Oligocene boundary begins 20 cm below the Shubuta–Bumpnose contact and ends 60 cm above the contact.

correspond to a highstand systems tract. The facies vary gradationally from a gray calcareous claystone in the upper Shubuta to black carbonaceous claystone intercalated with thin beds of fine quartz sandstone in the lower and middle Forest Hill, ending with a thick sandstone (not recovered in the core) at the top of the Forest Hill Formation. The Shubuta–Red Bluff contact is sharp and burrowed. The Red Bluff consists of black, fissile, fossiliferous claystones with sparse lenses of glauconitic sandstones. There is also a slight increase in the marine amorphous organic matter (Oboh and Yepes, 1995), although the dinocyst paleobathymetry does not show a significant deepening. This contact is indicative of a parasequence-bounding, minor flooding surface. The Marianna Limestone represents the transgressive systems tract.

7.3. #1 Ketler

The Eocene–Oligocene boundary is identified at 7.5 m, 3.7 m above the Shubuta–Red Bluff contact (Fig. 8). A maximum flooding surface is identified at 17 m, 7.6 composite units (0.106 Ma) older than the Eocene–Oligocene boundary, and 5.8 m below the Shubuta–Red Bluff contact (Fig. 13). This maximum flooding surface is characterized by a dark green calcareous claystone with abundant uvigerinids, a high values (3.6) of the dinocyst paleobathymetric index, and a high concentration of marine-derived organic matter (amorphous and dinocysts, Oboh and Yepes, 1995). It is also approximately 0.9 m above a pronounced gamma ray peak (Dockery et al., 1994). The Pachuta and lower Shubuta constitute a transgressive systems tract, whereas the upper Shubuta and Red

Bluff represent the overlying highstand systems tract. The transgressive systems tract is characterized by a gradation from silty, calcareous fossiliferous claystone in the middle and upper Pachuta to light green to gray, calcareous claystone with several levels of foraminifera-rich mudstones in the lower Shubuta. The highstand systems tract is characterized at the base by gray calcareous claystones (upper Shubuta). The Shubuta–Red Bluff contact is sharp and burrowed, and is similar in nature to the contact in the #1 Wayne core. It is interpreted as a minor flooding surface bounding a parasequence in the highstand systems tract.

7.4. R2089

In this short section shown in Fig. 14, the Eocene–Oligocene boundary occurs at 13.3 m measured from the base of the section, which is 0.1 m above the Shubuta–Red Bluff contact (Fig. 7). A maximum flooding surface is identified at 0 m, corresponding to 8.3 composite units, and is 0.116 Ma older than the Eocene–Oligocene boundary. A minor flooding surface is identified at the Shubuta–Red Bluff contact based on the increased abundance of *Deflandrea* group.

7.5. St. Stephens Quarry

Several hypotheses regarding the sequence stratigraphic interpretation of the St. Stephens Quarry section have been proposed by different researchers (see Fig. 2). A deep condensed section of 80 cm, containing a maximum flooding surface, begins 20 cm below the Shubuta–Bumpnose contact and ends 60 cm above it. This condensed section lasts for 13.7 composite units (0.19 Ma), and includes the Eocene–Oligocene boundary (Fig. 7). Evidences for this condensation and its paleobathymetry come from the dinocyst paleobathymetric index curve (Fig. 15), high abundance of the *Deflandrea* group, condensed dinocyst assemblages (see discussion on chronostratigraphy), and lithological characteristics. It consists of a thin, phosphatic, shell hash layer overlain by 60 cm of bluish, glauconitic calcareous clay and underlain by 20 cm of green calcareous clay (Pasley and Hazel, 1990). The maximum flooding surface probably corresponds to the thin, phosphatic shell layer which indicates maximum starvation and corresponds to the Shubuta–Bumpnose contact (Fig. 15). This interpretation basically agrees with Loutit et al. (1988) and Pasley and Hazel (1990) who located the condensed section at the same level based on lithology, foraminiferal paleoecology, a gamma ray peak, and palynofacies.

Pasley and Hazel (1995) identified a hiatus lasting 0.288 Ma at the Shubuta–Bumpnose contact, this hiatus being the product of starvation during the accumulation of the highstand deposits following the maximum flooding surface. They interpreted this contact as a sequence boundary which merged with the maximum flooding surface. Consequently, the first 60 cm of accumulation above the contact would correspond to lowstand deposits. However, it has been shown here that the paleobathymetric curves before and after the contact are very similar (sample 4.7 m: index 2.1; sample 5m: index 1.8, *Deflandrea* is abundant in both samples, contact is at 4.9 m.). Loutit et al. (1988) showed, based on foraminiferal paleoecology, that the maximum water depth occurred in the first 60 cm above the Shubuta–Bumpnose contact. If these sediments were deposited during the lowstand systems tract, a drastic change in paleobathymetry should be evident. Moreover, if a significant hiatus was present at the contact, the fossil assemblages immediately above it would show a gap in the fossil record as a consequence of erosion or nondeposition. The dinocyst fossil record, however, does not show a gap. Instead, it registers a condensation of datums in a short stratigraphic interval as a consequence of very slow input of sediment supply before, during, and after the maximum flooding surface. The graphic correlation of Pasley and Hazel (1995) probably shows a hiatus because of the relative time-coarseness of their composite section in comparison with ours. Whereas one composite unit in their scheme corresponds to 0.2 Ma, one unit in our study represents 0.014 Ma. Our entire composite section (units 50 to 120) would be compressed in only four units of theirs. This compression could create the effect of a hiatus.

A parasequence-bounding flooding surface is identified in the middle of the Bumpnose Limestone by the dinocyst paleobathymetric index and the abundance of *Deflandrea*. The Red Bluff–Mint Spring contact is characterized by a sequence bound-

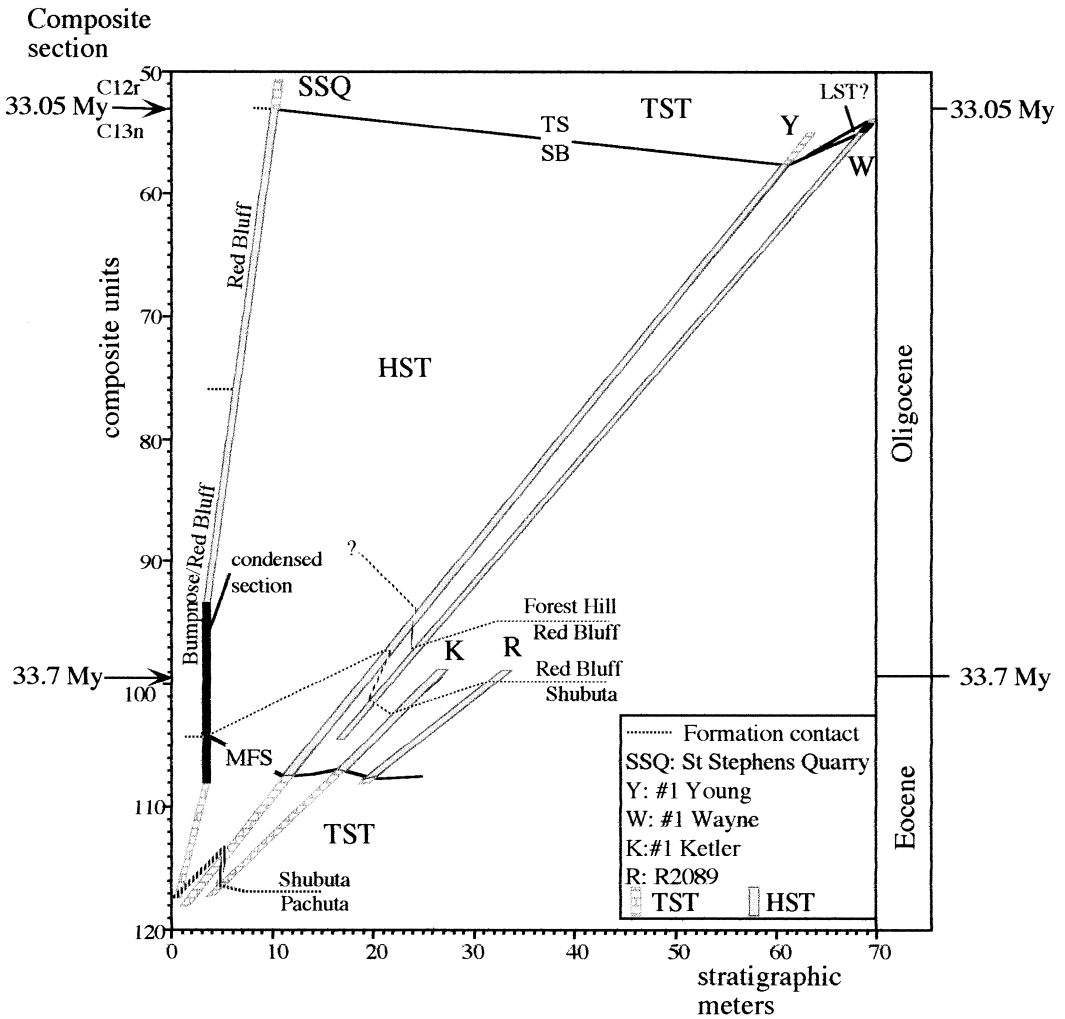

Fig. 16. Time (composite section) versus stratigraphic thickness for all the studied sections. Each composite unit is equivalent to 0.014 Ma. The sedimentation rates increase from southern Alabama (St. Stephens Quarry) to southern Mississippi (R2089). Refer to Fig. 1 for the location of the sections and Fig. 11 for key to sequence stratigraphy symbols.

ary which is merged with a transgressive surface. A sequence boundary is inferred based on similar reasons discussed above for the #1 Young core. Pasley and Hazel (1990, 1995) indicated that there was no evidence for a sequence boundary at this contact, because the contact climbed stratigraphically landward (from Alabama toward Mississippi). Our biostratigraphic data show the opposite, indicating that the contact is older in Mississippi and younger in Alabama (Fig. 16). Moreover, Tew and Mancini (1995) showed a number of localities in Mississippi and Alabama where this contact was sharp and disconformable, and contained broken and abraded shell material.

8. Concluding remarks

A correlation of all the studied sections (Figs. 16 and 17) shows that the positions of the maximum flooding surface in all of the sections, with the exception of the St. Stephens Quarry, are coeval and approximately 7.5 composite units (0.105 Ma) older than the Eocene–Oligocene boundary. At the

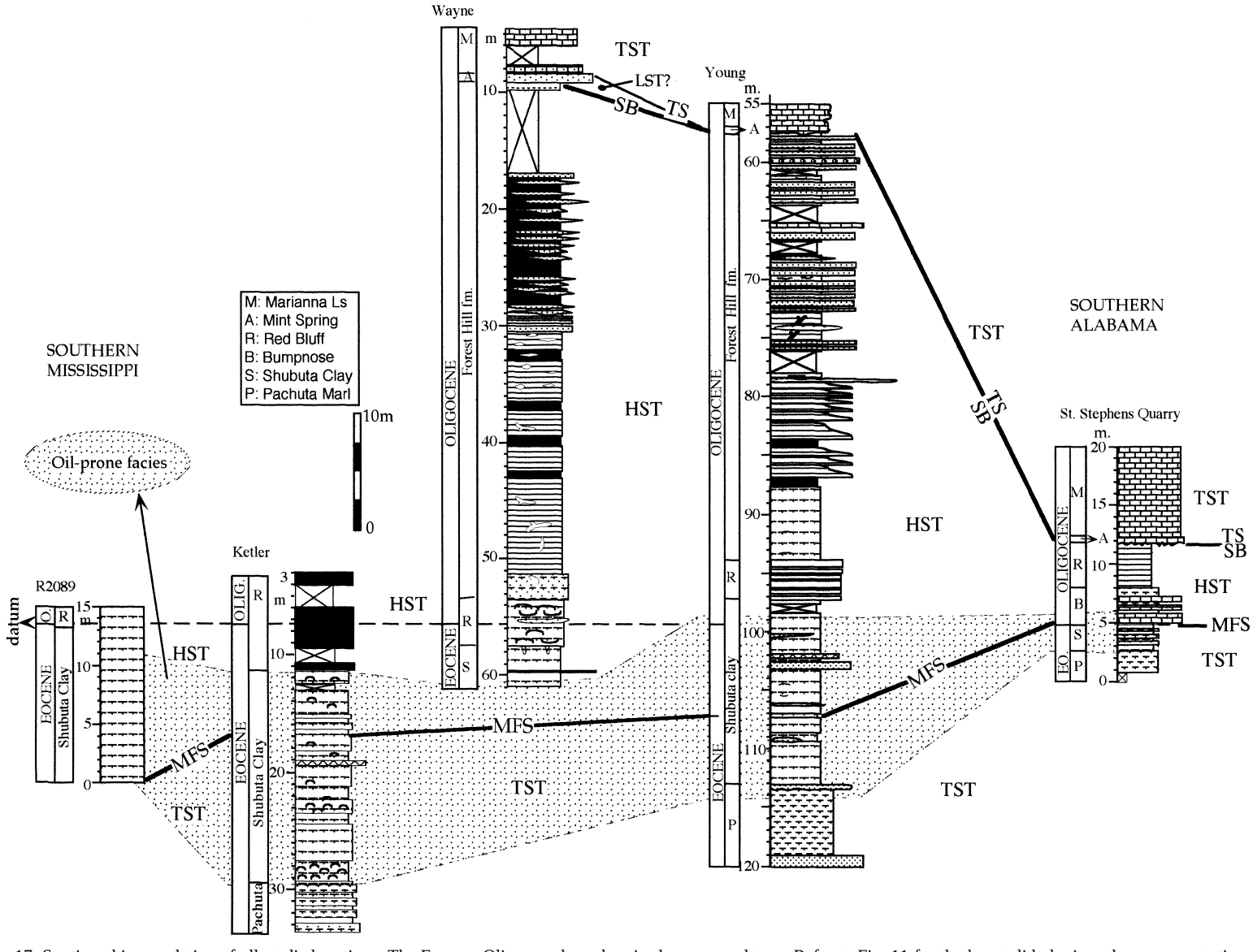

Fig. 17. Stratigraphic correlation of all studied sections. The Eocene–Oligocene boundary is chosen as a datum. Refer to Fig. 11 for the key to lithologic and sequence stratigraphy symbols. The sections increase in thickness toward southern Mississippi. The oil-rich organic facies (aquatic amorphous category) data were derived from Pasley and Hazel (1990) for the St. Stephens Quarry, from Oboh and Yepes (1995) for the #1 Wayne and #1 Ketler cores, and from this study for the #1 Young core and R2089 section.

St. Stephens Quarry section, this surface is three units (0.042 Ma) younger than the level at the other sections (Fig. 16). This maximum flooding surface occurs in the middle part of the Shubuta Clay in three sections in southern Mississippi (#1 Young, #1 Ketler and R2089) and at the Shubuta–Bumpnose contact at the St. Stephens Quarry section. In all four southern Mississippi sections, the Shubuta–Bumpnose contact is a minor flooding surface.

The Pachuta Marl and lower Shubuta Clay (entire Shubuta in southern Alabama) constitute a transgressive systems tract, whereas the upper Shubuta (in Mississippi) and Red Bluff–Bumpnose–Forest Hill Formations represent the overlying highstand systems tract. The Forest Hill–Mint Spring contact represents a sequence boundary which is merged with a transgressive surface. This contact is slightly older in the southern Mississippi sections. Isolated sandy patches of the Mint Spring in the #1 Wayne core are interpreted as representing a lowstand systems tract, whereas the marly Mint Spring (in other sections) and Marianna Limestone are constituents of a transgressive systems tract (Fig. 17).

The time–stratigraphic relationships stated above can be better understood in the time vs thickness diagram shown in Fig. 16. The condensed interval at the St. Stephens Quarry section corresponds to the accumulation of the Lower Oligocene highstand sediments (upper Shubuta + Red Bluff) in southern Mississippi. The continuation of normal sedimentation at the St. Stephens Quarry section appears to correspond to the accumulation of the Forest Hill in southern Mississippi. This result clearly shows that caution should be exercised when interpreting stratigraphic sequences based on formational contacts, because contacts are not time lines. Our result is contrary to previous claims that the Shubuta–Red Bluff contact corresponds to a sequence boundary (Dockery et al., 1994; Pasley and Hazel, 1995). In addition, Tew and Mancini (1995) noted that the Forest Hill-filled channels at the Shubuta–Vicksburg Group contact, reported by Dockery (1990), were the product of stochastic processes associated with the progradation of the shoreline during the highstand.

Rates of accumulation increased from southern Alabama (St. Stephens Quarry) to the farther section (R2089) in southern Mississippi (Figs. 1, 16 and 17). Areas in southeastern Mississippi experienced more rapid and prograding clastic sedimentation, whereas shelf-edge sediments were deposited much more slowly by longshore transport in the St. Stephens Quarry area.

Our sequence stratigraphic interpretation is in general agreement with previous studies for the Pachuta–Forest Hill interval (corresponds to the TE 3.3 depositional sequence of Baum and Vail, 1988, and the TAGC 4.3 depositional sequence of Tew and Mancini, 1995), although there are four distinct differences. First, the maximum flooding surface of the Pachuta–Forest Hill sequence is in the middle of the Shubuta Clay in southern Mississippi but at the Shubuta–Bumpnose contact in the St. Stephens Quarry section. Second, the age of this maximum flooding surface is latest Eocene. Third, the lower 60 cm of the Bumpnose Limestone in the St. Stephens Quarry section accumulated during the deposition of the upper Shubuta and Red Bluff in southern Mississippi. And fourth, the sequence boundary at the Forest Hill–Mint Spring contact does not correlate with the TA 4.3/TA 4.4 sequence boundary of Haq et al. (1988). Therefore, the terminology TA 4.3 and TA 4.4 depositional sequences should not be applied to this stratigraphic interval in the study area.

Acknowledgements

We would like to thank Norman Frederiksen and Lucy Edwards (U.S. Geological Survey) for loan of the St. Stephens Quarry and R2089 samples, and Larry Fearn (Mobil Exploration and Producing) for providing the core samples, and Mobil for permission to publish the results from the Mississippi cores. Thanks to Martin Farley, David Pocknall and Lucy Edwards for reviewing an earlier version of the manuscript. We are also grateful to journal reviewers Henk Brinkhuis and Graham Williams for their detailed reviews which have greatly improved this paper. This research was funded by National Science Foundation Grant No. EAR-9405154 to FEO. CJ thanks to Colciencias for its support during the research.

Appendix A. Previous paleoecological interpretations for dinocysts, acritarchs, and algae found in this study

Taxa	Ecological interpretation	Reference
Achomosphaera sp.	lower paleolatitudes	Brinkhuis and Biffi (1993)
Achomosphaera	middle to outer neritic	Brinkhuis et al. (1992)
Achomosphaera	open marine neritic or its influence by offshore transport	Brinkhuis (1994)
Achomosphaera	nearshore shallow water	Brinkhuis and Zachariasse (1988)
Achomosphaera	transgressive tendency, higher% deeper water	Köthe (1990)
Achomosphaera	open marine, most abundant during transgressions	Islam (1984)
Achomosphaera alcicornu	open sea	Downie et al. (1971)
Apteodinium spp.	marginal marine	Zevenboom et al. (1994)
Areosphaeridium diktyoplokus	40º–60ºN present-day latitude	Williams and Bujak (1977)
Enneadocysta	increased salinity	Köthe (1990)
Enneadocysta multicornuta	Florida–West Africa–southern England–Grand Banks	Williams and Bujak (1977)
E. pectiniformis and allied taxa	neritic	Brinkhuis (1994)
Ascostomocystis (acritarch)	highest abundances in inner neritic	Brinkhuis (1994)
Ascostomocystis (acritarch)	cosmopolitan	Brinkhuis (1994)
Batiacasphaera	offshore	Brinkhuis and Zachariasse (1988)
Cannosphaeropsis	oceanic	Brinkhuis and Biffi (1993)
Charlesdowniea	lagoonal, estuarine or brackish	Islam (1984)
Charlesdowniea coleothrypta	more offshore, high diversity, low dominance	Goodman (1979)
Cleistosphaeridium	normal marine but shallow water	Köthe (1990)
Cordosphaeridium	open marine	Köthe (1990)
Cordosphaeridium	open marine, most abundant during transgressions	Islam (1984)
Cordosphaeridium inodes	open sea	Downie et al. (1971)
Cribroperidinium tenuitabulatum	deep and cool water	Köthe (1990)
Cyclopsiella (acritarch)	highest abundances in inner neritic, cosmopolitan	Brinkhuis (1994)
Deflandrea	lagoonal, estuarine or brackish	Islam (1984)
Deflandrea	heterotrophic, reflects an excess of nutrients	Brinkhuis et al. (1992)
Deflandrea	estuarine	Downie et al. (1971)
Deflandrea	lagoonal, estuarine, or brackish	Köthe (1990)
Deflandrea spp.	high primary production	Brinkhuis (1994)
Deflandrea phosphoritica	more inshore, low diversity, high dominance	Goodman (1979)
Pediastrum (alga)	estuarine	Brown and Downie (1984)
Glaphyrocysta	open marine, high energy	Islam (1984)
Glaphyrocysta	(open marine) inner neritic water masses	Brinkhuis (1994)
Glaphyrocysta	inner to middle neritic	Brinkhuis et al. (1992)
Glaphyrocysta	nearshore	Brinkhuis and Zachariasse (1988)
Glaphyrocysta	open marine	Köthe (1990)
Glaphyrocysta	warm water	Köthe (1990)
Hemiplacophora semilunifera	outer neritic taxon	Brinkhuis (1994)
H. semilunifera	lower paleolatitudes	Brinkhuis and Biffi (1993)
Homotryblium	marginal marine	Zevenboom et al. (1994)
Homotryblium (mainly *H. plectilum*)	increased salinity	Köthe (1990)
Homotryblium plectilum	open sea conditions, 40 or more species	Liengjarern et al. (1980)
Homotryblium sp.	lower paleolatitudes	Brinkhuis and Biffi (1993)
Homotryblium spp.	restricted marine to inner neritic in low to middle latitudes	Brinkhuis (1994)
Homotryblium	lagoon and equatorial	Dale (1996)
Hystrichokolpoma rigaudiae	more inshore	Goodman (1979)
Impagidinium	oceanic, 1–2% in neritic/oceanic boundary, stable salinity 35‰	Dale (1996)
Impagidinium	oceanic	Zevenboom et al. (1994)

Appendix A (continued)

Taxa	Ecological interpretation	Reference
Impagidinium (5 species)	outer neritic–oceanic	Wrenn and Kokinos (1986)
Impagidinium spp. excluding *I. pallidum* and *I. vellorum*	warm	Zevenboom et al. (1994)
I. aculeatum (and related species)	outermost shelf, slope, rise and abyssal sediments	Wall et al. (1977)
I. aculeatum (and related species)	tropical–subtropical	Wall et al. (1977)
Impagidinium dispertitum	lower paleolatitudes	Brinkhuis and Biffi (1993)
Impagidinium pallidum + *I. vellorum*	cold	Zevenboom et al. (1994)
Impagidinium spp.	outer neritic to oceanic	Edwards and Andrle (1992); Mudie and Harland (1996)
Impagidinium spp.	oceanic	Harland (1983)
Impagidinium	oceanic	Brinkhuis and Biffi (1993); Brinkhuis et al. (1992)
Lingulodinium spp.	marginal marine	Zevenboom et al. (1994)
Lingulodinium machaerophorum	more offshore, high diversity, low dominance	Goodman (1979)
Lingulodinium	nearshore	Brinkhuis et al. (1992)
Lingulodinium	euryhaline	Islam (1984)
Nematosphaeropsis	oceanic	Zevenboom et al. (1994); Brinkhuis et al. (1992); Brinkhuis and Biffi (1993)
Nematosphaeropsis	neritic–oceanic, dominate oceanic assemblage	Dale (1996)
Nematosphaeropsis balcombiana	neritic–oceanic, more abundance in slope and rise	Wall et al. (1977)
Nematosphaeropsis labyrinthea	outer neritic–oceanic, cosmopolitan	Harland (1983)
Nematosphaeropsis spp.	temperate	Zevenboom et al. (1994)
Operculodinium	mainly neritic, cosmopolitan	Brinkhuis et al. (1992)
Operculodinium	euryhaline	Islam (1984)
Operculodinium centrocarpum	shelf	Brown and Downie (1984)
O. centrocarpum	acme at neritic–oceanic boundary	Dale (1996)
O. centrocarpum	equatorial to polar	Dale (1996); Edwards and Andrle (1992); Harland (1983)
O. centrocarpum	relatively most abundant offshore	Davey and Rogers (1975)
O. centrocarpum	warmer water	Davey and Rogers (1975)
O. centrocarpum	nutrient-poor water	Davey and Rogers (1975)
O. centrocarpum	estuarine to oceanic	Edwards and Andrle (1992)
O. centrocarpum	widespread in North Atlantic, most common in outer neritic	Harland (1983)
O. centrocarpum	outer coastal zone (30–50 m depth)	Morzadec (1983, 1992)
O. centrocarpum	tends to be more abundant in shelf sediments	Wall et al. (1977)
O. centrocarpum	abundance tends to decrease tropicwards	Wall et al. (1977)
O. centrocarpum	cosmopolitan	Williams and Bujak (1977); Williams (1971)
O. centrocarpum	inner neritic–oceanic	Wrenn and Kokinos (1986)
O. centrocarpum	restricted marine to open marine neritic water masses	Brinkhuis (1994)
Spiniferites	middle to outer neritic	Brinkhuis et al. (1992)
Spiniferites (mainly *S. ramosus*)	open marine neritic or its influence by offshore transport	Brinkhuis (1994)
Spiniferites	abundance peak in upper shelf	Hultberg and Malmgren (1986)
Spiniferites	nearshore shallow water	Brinkhuis and Zachariasse (1988)
Spiniferites	transgressive tendency, higher% in deeper water	Köthe (1990)
Spiniferites	open marine, most abundant during transgressions	Islam (1984)
Spiniferites spp.	estuarine	Lenoir and Hart (1988)
Spiniferites ramosus	open sea	Downie et al. (1971)
S. ramosus	open sea conditions	Liengjarern et al. (1980)
S. ramosus	estuarine to outer neritic, broad thermal tolerance	Edwards and Andrle (1992)

Appendix A (continued)

Taxa	Ecological interpretation	Reference
S. ramosus	neritic, cosmopolitan	Harland (1983)
S. ramosus	inner–outer neritic	Wrenn and Kokinos (1986)
S. ramosus (sensu Davey, 1971)	estuarine–neritic, tropical–subtropical	Wall et al. (1977)
S. ramosus (sensu Wall and Dale, 1970)	maximum abundance in estuaries or innermost shelf zone	Wall et al. (1977)
S. ramosus (sensu Wall and Dale, 1970)	tropical–subtropical	Wall et al. (1977)
Spiniferites ramosus subsp. *ramosus*	most abundant nearshore	Davey and Rogers (1975)
Spiniferites ramosus subsp. *ramosus*	colder water, upwelling, nutrient-rich water	Davey and Rogers (1975)
Spiniferites spp.	estuarine, low cyst diversity	Brown and Downie (1984)
Spiniferites spp.	neritic	Harland (1983)
Spiniferites pseudofurcatus	marginal marine	Zevenboom et al. (1994)
S. pseudofurcatus	open marine neritic	Brinkhuis (1994)
Systematophora spp.	marginal marine	Zevenboom et al. (1994)
Systematophora placacantha	open marine, warm water	Köthe (1990)
Systematophora	all marine environments, global	Brinkhuis (1994)
Tectatodinium pellitum	neritic	Dale (1996)
T. pellitum	estuarine to oceanic	Edwards and Andrle (1992)
T. pellitum	cool-temperate to warm-temperate	Edwards and Andrle (1992)
T. pellitum	inner to outer neritic	Harland (1983); Mudie and Harland (1996); Wrenn and Kokinos (1986)
T. pellitum	south-temperate to subtropical in North Atlantic	Harland (1983)
T. pellitum	cool-temperate to tropical	Mudie and Harland (1996)
T. pellitum	more common from outer shelf and slope rise, cosmopolitan	Wall et al. (1977)
T. pellitum	warm water	Head (1994)
Wetzeliella	lagoonal, estuarine or brackish	Islam (1984)
Wetzeliella	occasionally abundant in shelf	Brown and Downie (1984)
Wetzeliella lunaris	more inshore	Goodman (1979)
Wetzeliella complex	middle latitudes	Goodman (1987)
Wetzeliella	estuarine	Downie et al. (1971)
Wetzeliella	lagoonal, estuarine, or brackish, tolerant of reduced salinity	Köthe (1990)

References

Batten, D.J., 1996. Palynofacies and palaeoenvironmental interpretation. In: Jansonius, J., MacGregor, D.C. (Eds.), Palynology: Principles and Applications. American Association of Stratigraphic Palynologists Foundation, Dallas, TX, pp. 1011–1064.

Baum, G.R., Vail, P.R., 1988. Sequence stratigraphic concepts applied to Paleogene outcrops, Gulf and Atlantic Coastal basins. In: Wilgus, C.K., Hastings, B.S., Kendall, C.G.St.C., Posamentier, H.W., Ross, C.A., Van Wagoner, J.C. (Eds.), Sea-Level Changes: An Integrated Approach. Soc. Econ. Paleontol. Mineral. Spec. Publ. 42, 309–327.

Berggren, W.A., Kent, D.V., Swisher, C.C. II, Aubry, M., 1995. A revised Cenozoic Geochronology and Chronostratigraphy. In: Berggren, W.A., Kent, D.V., Aubry, M.P., Hardenbol, J. (Eds.), Geochronology Time Scales and Global Stratigraphic Correlation. Soc. Econ. Paleontol. Mineral. Spec. Publ. 54, 129–212.

Brinkhuis, H., 1992. Late Paleogene dinoflagellate cysts with special reference to the Eocene/Oligocene boundary. In: Prothero, D.R., Berggren, W.A. (Eds.), Eocene–Oligocene Climatic and Biotic Evolution. Princeton University Press, Princeton, NJ, pp. 327–340.

Brinkhuis, H., 1994. Late Eocene to early Oligocene dinoflagellate cysts from the Priabonian type-area (Northeast Italy): biostratigraphy and paleoenvironmental interpretation. Palaeogeogr., Palaeoclimatol., Palaeoecol. 107, 121–163.

Brinkhuis, H., Biffi, U., 1993. Dinoflagellate cyst stratigraphy of the Eocene/Oligocene transition in central Italy. Mar. Micropaleontol. 22, 131–183.

Brinkhuis, H., Visscher, H., 1995. The upper boundary of the Eocene Series: a reappraisal based on dinoflagellate cyst biostratigraphy and sequence stratigraphy. In: Berggren, W.A., Kent, D.V., Aubry, M.P., Hardenbol, J. (Eds.), Geochronology Time Scales and Global Stratigraphic Correlation. Soc. Econ. Paleontol. Mineral. Spec. Publ. 54, 295–304.

Brinkhuis, H., Zachariasse, W.J., 1988. Dinoflagellate cysts,

sea level changes and planktonic foraminifers across the Cretaceous–Tertiary boundary at El Haria, Northwest Tunisia. Mar. Micropaleontol. 13, 153–191.

Brinkhuis, H., Powell, A.J., Zevenboom, D., 1992. High-resolution dinoflagellate cyst stratigraphy of the Oligocene/Miocene transition interval in north-west and central Italy. In: Head, M.J., Wrenn, J.H. (Eds.), Neogene and Quaternary Dinoflagellate Cysts and Acritarchs. American Association of Stratigraphic Palynologists Foundation, Dallas, pp. 219–258.

Brown, S., Downie, C., 1984. Dinoflagellate cyst biostratigraphy of late Paleogene and Early Eocene sediments from Holes 552, 553A, and 555, Leg 81, Deep Sea Drilling Project (Rockall Plateau). Proc. DSDP, Init. Rep. 81, 565–579.

Bybell, L.M., 1982. Late Eocene to early Oligocene calcareous nannofossils in Alabama and Mississippi. Trans. Gulf Coast Assoc. Geol. Soc. 32, 295–302.

Bybell, L.M., Poore, R.Z., 1983. Reworked Hantkenina specimens at Little Stave Creek, Alabama. Trans. Gulf Coast Assoc. Geol. Soc. 33, 253–256.

Châteauneuf, J.-J., 1983. Dinokystes et milieux confines du Paléogène du bassin de Paris. Sci. Geol. Bull 36, 223–230.

Dale, B., 1996. Dinoflagellate cyst ecology: modeling and geological applications. In: Jansonius, J., MacGregor, D.C. (Eds.), Palynology: Principles and Applications. American Association of Stratigraphic Palynologists Foundation, Dallas, pp. 1249–1275.

Davey, R., 1971. Palynology and palaeo-environmental studies, with special reference to the continental shelf sediments of South Africa. In: Farinacci, A. (Ed.), Proceedings of the 2nd Planktonic Conference. Tecnoscienza, Roma, pp. 331–347.

Davey, R.J., Rogers, J., 1975. Palynomorph distribution in recent offshore sediments along two traverses off southwest Africa. Mar. Geol. 18, 213–225.

Dockery, D.T. III, 1990. The Eocene Oligocene boundary in the northern Gulf — a sequence boundary. GCSSEPM Foundation, 11th Annual Research Conference, Programs and Extended Abstracts, pp. 141–150.

Dockery III, D.T., Thompson, D.E., Stephen, L.I., 1994. The Mobil-Mississippi Office of Geology Core-Hole Project. Mississippi Geol. 15, 8–13.

Downie, C., Hussain, M.A., Williams, G.L., 1971. Dinoflagellate cyst and acritarch associations in the Paleogene of southeast England. Geosci. Man 3, 29–35.

Edwards, L.E., 1989. Supplemented graphic correlation: a powerful tool for paleontologists and nonpaleontologists. Palaios 4, 127–143.

Edwards, L.E., Andrle, V.A., 1992. Distribution of selected dinoflagellate cysts in modern marine sediments. In: Head, M.J., Wrenn, J.H. (Eds.), Neogene and Quaternary Dinoflagellate Cysts and Acritarchs. American Association of Stratigraphic Palynologists Foundation, Dallas, pp. 259–288.

Galloway, W.E., 1989. Genetic stratigraphic sequences in basin analysis, II. Application to Northwest Gulf of Mexico Cenozoic Basin. Am. Assoc. Pet. Geol. Bull. 73, 143–154.

Galloway, W.E., Bebout, D.G., Fisher, W.L., Dunlap, J.B., Cabrera-Castro, R., LUGO-Riviera, J.E., Scott, T.M., 1991. Cenozoic. In: Salvador, A. (Ed.), The Gulf of Mexico Basin. The Geology of North America Volume J, Geological Society of America, Boulder, CO, pp. 245–324.

Goodman, D.K., 1979. Dinoflagellate 'communities' from the lower Eocene Nanjemoy Formation of Maryland, U.S.A. Palynology 3, 169–190.

Goodman, D.K., 1987. Dinoflagellate cysts in ancient and modern sediments. Bot. Monogr. 21, 649–722.

Gregory, W.A., Hart, G.F., 1992. Towards a predictive model for the palynologic response to sea-level changes. Palaios 7, 3–33.

Habib, D., Miller, J.A., 1989. Dinoflagellate species and organic facies evidence of marine transgression and regression in the Atlantic coastal plain. Palaeogeogr., Palaeoclimatol., Palaeoecol. 74, 23–47.

Haq, B.U., Hardenbol, J., Vail, P.R., 1988. Mesozoic and Cenozoic chronostratigraphy and cycles of sea-level changes. In: Wilgus, C.K., Hastings, B.S., Kendall, C.G.St.C., Posamentier, H.W., Ross, C.A., Van Wagoner, J.C. (Eds.), Sea-Level Changes: An Integrated Approach. Soc. Econ. Paleontol. Mineral. Spec. Publ. 42, 72–108.

Harland, R., 1983. Distribution maps of recent dinoflagellate cysts in bottom sediments from the North Atlantic Ocean and adjacent seas. Palaeontology 26, 321–387.

Hazel, J.E., Mumma, M.D., Huff, W.J., 1980. Ostracode biostratigraphy of the Lower Oligocene (Vicksburgian) of Mississippi and Alabama. Trans. Gulf Coast Assoc. Geol. Soc. 30, 361–401.

Head, M.J., 1994. Morphology and paleoenvironmental significance of the Cenozoic dinoflagellate genera *Tectatodinium* and *Habibacysta*. Micropaleontology 40, 289–321.

Head, M.J., Norris, G., 1989. Palynology and dinocyst stratigraphy of the Eocene and Oligocene in ODP Leg 105, Hole 647A, Labrador Sea. Proc. ODP Sci. Results 105, 515–550.

Hultberg, S.U., Malmgren, B.A., 1986. Dinoflagellate and planktonic foraminiferal paleobathymetrical indices in the Boreal uppermost Cretaceous. Micropaleontology 32, 316–323.

Islam, M.A., 1984. A study of Early Eocene palaeoenvironments in the Isle of Sheppey as determined from microplankton assemblage composition. Tertiary Res. 6, 11–21.

Jaramillo, C., 1995. Dinoflagellate Cyst Biostratigraphy and Palynofacies of the Late Eocene–Early Oligocene in Southern Mississippi and Alabama, U.S. Gulf Coast. MS. Thesis, Univ. of Missouri–Rolla, Rolla, MO, 97 pp.

Keller, G., 1985. Eocene and Oligocene stratigraphy and erosional unconformities in the Gulf of Mexico and Gulf Coast. J. Paleontol. 59, 882–903.

Köthe, A., 1990. Paleogene dinoflagellates from northwest Germany — biostratigraphy and Palaeoenvironments. Geol. Jahrb. A118, 3–111.

Kovach, W.L., 1989. Comparisons of multivariate analytical techniques for use in Pre-Quaternary plant paleoecology. Rev. Palaeobot. Palynol. 60, 255–282.

Lenoir, E.A., Hart, G.F., 1988. Palynofacies of some Miocene sands from the Gulf of Mexico, offshore Louisiana, U.S.A. Palynology 12, 151–166.

Lentin, J.K., Williams, G.L., 1993. Fossil dinoflagellates: index to genera and species. Am. Assoc. Stratigr. Palynol. Contrib. Ser. 28, 1–855.

Liengjarern, M., Costa, L., Downie, C., 1980. Dinoflagellate cysts from the Upper Eocene–Lower Oligocene of the Isle of Wight. Palaeontology 23, 475–499.

Lorente, M., 1986, Palynology and palynofacies of the upper Tertiary in Venezuela. Dissertationes Botanicae 99, 222 pp.

Loutit, T.S., Baum, G.R., Wright, R.C., 1983. Eocene–Oligocene sea level changes as reflected in Alabama outcrop sections. Am. Assoc. Pet. Geol. Bull. 67, 506.

Loutit, T.S., Handenbol, J., Vail, P.R., Baum, G.R., 1988. Condensed sections: the key to age determination and correlation of continental margin sequences. In: Wilgus, C.K., Hastings, B.S., Kendall, C.G.St.C., Posamentier, H.W., Ross, C.A., Van Wagoner, J.C. (Eds.), Sea-Level Changes: An Integrated Approach. Soc. Econ. Paleontol. Mineral. Spec. Publ. 42, 183–213.

Mancini, E.A., 1979. Eocene–Oligocene boundary in southwest Alabama. Trans. Gulf Coast Assoc. Geol. Soc. 29, 282–286.

Miller, K.G., Thompson, P.R., Kent, D.V., 1993. Integrated late Eocene–Oligocene stratigraphy of the Alabama coastal plain: correlation of hiatuses and stratal surfaces to glacioeustatic lowerings. Paleoceanography 8, 313–331.

Morzadec, M.T., 1983. Intéret des kistes de dinoflagelles pour l'établissement de réconstitution paléogéographique: exemple du Golfe de Gabes (Tunisie). Cah. Micropaleontol. 1983 (4), 15–22.

Morzadec, M.T., 1992. Upper Pleistocene and Holocene dinoflagellate cyst assemblages in marine environments of the Mediterranean Sea and the northwest Atlantic Coast of France. In: Head, M.J., Wrenn, J.H. (Eds.), Neogene and Quaternary Dinoflagellate Cysts and Acritarchs. American Association of Stratigraphic Palynologists Foundation, Dallas, pp. 121–132.

Mudie, P.J., Harland, R., 1996. Aquatic Quaternary. In: Jansonius, J., McGregor, D.C. (Eds.), Palynology: Principles and Applications. American Association of Stratigraphic Palynologists Foundation, Dallas, pp. 843–877.

Muller, J., 1959. Palynology of the recent Orinoco delta and shelf sediments: reports of the Orinoco Shelf Expedition. Micropaleontology 5, 1–32.

Oboh, F.E., 1992. Multivariate statistical analyses of palynodebris from the middle Miocene of the Niger Delta and their environmental significance. Palaios 7, 559–573.

Oboh, F.E., Yepes, O., 1995. Palynofacies analysis of #1 Ketler and #1 Wayne cores. Mobil Exploration Internal Report.

Pasley, M.A., Hazel, J.E., 1990. Use of organic petrology in graphic correlation of biostratigraphic data in sequence stratigraphic interpretations: example from the Eocene–Oligocene boundary section, St. Stephens Quarry, Alabama. Trans. Gulf Coast Assoc. Geol. Soc. 40, 661–683.

Pasley, M.A., Hazel, J.E., 1995. Revised sequence stratigraphic interpretation of the Eocene–Oligocene boundary interval, Mississippi and Alabama, Gulf Coast Basin, USA. J. Sediment. Res. B 65, 160–169.

Pielou, E.C., 1984. The Interpretation of Ecological Data. Wiley, New York, 263 pp.

Posamentier, H.W., Allen, G.P., James, D.P., Tesson, M., 1992. Forced regressions in a sequence stratigraphic framework: concepts, examples and exploration significance. Am. Assoc. Pet. Geol. Bull. 76, 1687–1709.

Powell, A.J., Brinkhuis, H., Bujak, J.P., 1996. Upper Paleocene–lower Eocene dinoflagellate cyst sequence biostratigraphy od southeast England. In: O'B. Knox, R.W., Cirfield, R.M., Dunay, R.E. (Eds.), Correlation of the Early Paleogene in Northwest Europe. Geol. Soc. London Spec. Publ. 101, 145–183.

Shaw, A.B., 1964. Time in Stratigraphy. MacGraw-Hill, New York, 365 pp.

Siesser, W.G., 1983. Paleogene calcareous nannoplankton biostratigraphy: Mississippi, Alabama and Tennessee. Mississippi Bur. Geol. Bull. 125, 1–61.

Siesser, W.G., Fitzgerald, B.G., Kronman, D.J., 1985. Correlation of Gulf Coast provincial Paleogene stages with European standard stages. Geol. Soc. Am. Bull. 96, 827–831.

Sokal, R.R., Michener, C.D., 1958. A statistical method for evaluating systematic relationships. Univ. Kansas Sci. Bull. 38, 1409–1438.

Stover, L.E., Williams, G.L., 1995. A revision of the Paleogene dinoflagellate genera *Areosphaeridium* Eaton 1971 and *Eatonicysta* Stover and Evitt 1978. Micropaleontology 41, 97–141.

Systat, 1992. SYSTAT 5 for the Macintosh, Version 5.2.1. Copyright, SYSTAT Inc., 603 Main Street, Evanston, IL 60202.

Tew, B.H., Mancini, E.A., 1995. An integrated lithostratigraphic, biostratigraphic, and sequence stratigraphic approach to paleogeographic reconstruction: examples from the Upper Eocene and Lower Oligocene of Alabama and Mississippi. Palaios 10, 133–153.

Traverse, A., 1988. Paleopalynology. Allen and Unwin, Boston, MA, 600 pp.

Traverse, A., Ginsburg, R.N., 1966. Palynology of the surface sediments of the Great Bahama Bank, as related to water movement and sedimentation. Mar. Geol. 4, 417–459.

Van Vergen, P., Janssen, N., Alferink, J., Kerp, J., 1990. Recognition of organic matter types in standard palynological slides. Meded. Rijks Geol. Dienst 45, 1–23.

Wall, D., Dale, B., 1970. Living hystrichosphaerid dinoflagellate from Bermuda and Puerto Rico. Mar. Micropaleontol. 16, 47–58.

Wall, D., Dale, B., Lohmann, G.P., Smith, W.K., 1977. The environmental and climatic distribution in modern marine sediments from regions in the North and South Atlantic oceans and adjacent seas. Mar. Micropaleontol. 2, 121–200.

Williams, D.B., 1971. The occurrence of dinoflagellates in marine sediments. In: Funnell, B.M., Riedel, W.R. (Eds.), The Micropaleontology of Oceans. Cambridge University Press, Cambridge, pp. 231–243.

Williams, G.L., Bujak, J.P., 1977. Distribution patterns of some North Atlantic Cenozoic dinoflagellate cysts. Mar. Micropaleontol. 2, 223–233.

Wrenn, J.H., Kokinos, J.P., 1986. Preliminary comments on Miocene through Pleistocene Dinoflagellate Cysts from De Soto Canyon, Gulf of Mexico. Am. Assoc. Stratigr. Palynol. Contrib. Ser. 17, 169–225.

Zevenboom, D., Brinkhuis, H., Visscher, H., 1994. Dinoflagellate cyst palaeoenvironmental analysis of the Oligocene/Miocene transition in northwest and central Italy. G. Geol. Ser. 3, 56, 155–169.